

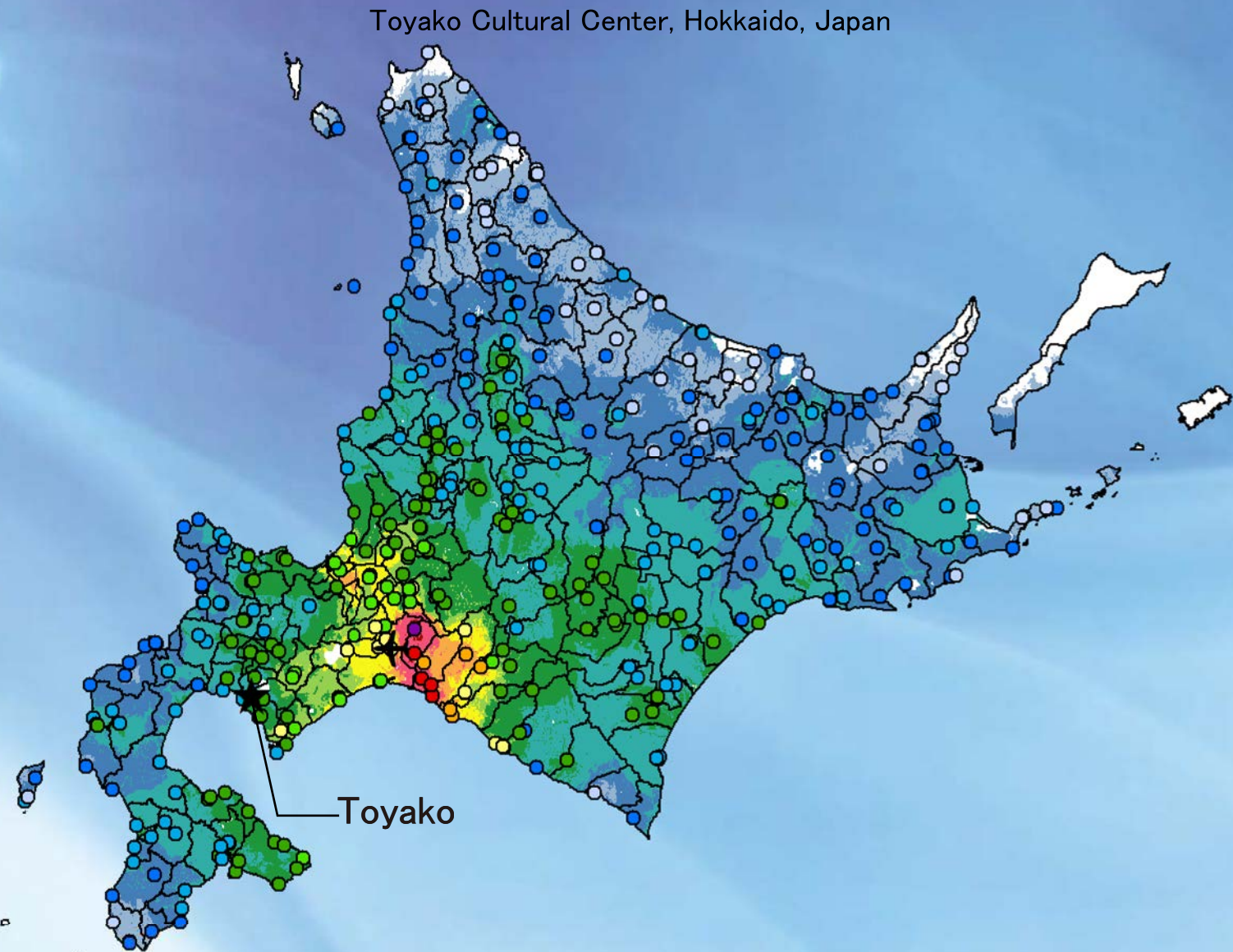


The 2019 Japan–NewZealand–Taiwan Seismic Hazard Workshop

Abstract Proceedings

4 – 6 November, 2019

Toyako Cultural Center, Hokkaido, Japan



The 2019 Japan–NewZealand–Taiwan Seismic Hazard Workshop

Abstract Proceedings

4 – 6 November, 2019

■ Front cover

Distribution of Seismic Intensity of the 2018 Hokkaido Eastern Iburi Earthquake estimated by J-RISQ.

This figure was automatically released in about 10 minutes after the P-wave arrival.

It is based on the more than 400 online seismic records in Hokkaido.

<http://www.j-risq.bosai.go.jp/report/en/>

Legend

Seismic Intensity

- 1
- 2
- 3
- 4
- 5-
- 5+
- 6-
- 6+
- 7

■ Back cover

Upper left: Hokkaido Toyako summit commemorative museum

Upper right: Lake Toya

Lower left: Mount Showashinzan

Lower right: Landslide in Atsuma-town caused by the 2018 Iburi Earthquake



The 2019 Japan–NewZealand–Taiwan Seismic Hazard Workshop

Abstract Proceedings

4 – 6 November, 2019

Toyako Cultural Center, Hokkaido, Japan

Preface

Welcome to the 2019 Japan-New Zealand-Taiwan Seismic Hazard Assessment (SHA) meeting at Lake Toya (Toyako), Hokkaido. This is a third cycle of Group of SHA workshops after the first of 2013 Sendai and the second of 2016 Beppu. The Group of SHA (G-SHA) workshop initiated by Japan-China-Korea strategic program after Wenchuan earthquake, inherited by Taiwan Earthquake Model (TEM) and Japan (NIED) after Tōhoku earthquake, as well as joined by New Zealand (GNS Science) from 2014.

Recently destructive earthquakes occurred in the G-SHA countries as listed, which hints epistemic uncertainty of probabilistic SHA and sustainability of G-SHA workshop.

2008 Wenchuan earthquake, China	(M=7.9, 87,587 fatalities)
2011 Tōhoku earthquake and tsunami, Japan	(M=9.0, 19,689 fatalities)
2011 Christchurch earthquake, New Zealand	(M=6.2, 185 fatalities)
2016 Meinong earthquake, Taiwan	(M=6.6, 117 fatalities)
2016 Kumamoto earthquake, Japan	(Mj=7.3, 273 fatalities)
2016 Kaikoura M7.9 earthquake, New Zealand	(M=7.9, 2 fatalities)
2018 Hualien earthquake, Taiwan	(M=6.4, 17 fatalities)
2018 Osaka-Fu Hokubu earthquake, Japan	(Mj=6.1, 6 fatalities)
2018 Hokkaido Eastern Iburi earthquake, Japan	(Mj=6.7, H=37km, 43 fatalities)
2019 Hualien earthquake, Taiwan	(M=6.1, 1 fatalities)

Toyako is near an epicenter of the 2018 Hokkaido Eastern Iburi earthquake which was much deep focus than usual inland earthquakes. We choose it as the G-SHA workshop venue and try to aware of the complexities of earthquake sources and challenges of the modelling of seismic hazard, especially for the triple countries where the island-arc of plate boundaries located in. We also arrange a series of field trips for 1) Mt. Usu volcano eruption and damage traces; 2) active fault investigation; and 3) Iburi earthquake landslide damage.

Through this ongoing series of workshops, we aim to sophisticate the topics such as earthquake source characterization, ground motion simulation and prediction, subduction zone modelling and risk assessment. Some newer research topics will also be focus on in this year G-SHA workshop. Colleagues from Building Research Institute Japan, Yonsei university Korea, USGS, and Global Earthquake Model Foundation (GEM) will share their ideas and participate G-SHA collaborations.

Conveners

Ken XS Hao, Takahiro Maeda & Hiroyuki Fujiwara (NIED)

Field Trip Leader

Takashi Azuma (GSJ, AIST)

Contents

Program on 4 November 2019	ii
Program on 5 November 2019	iii
Program poster session	iv
Program on 6 November 2019.....	v
Abstract.....	<i>1-54</i>

Program on 4 November 2019 (Monday)

Location: Toyako Cultural Center

AM

	8:30-9:00		Registration
	9:00-9:15		Opening ceremony
Session 1: Current status of Seismic hazard Assessment for each country (1)			
			Chair : Ken Xiansheng Hao
Hiroyuki Fujiwara	9:15-9:30	1A- 1	National Seismic Hazard Maps for Japan and its application to improve disaster resilience
Matt Gerstenberger	9:30-9:45	1A- 2	Recent progress and future plans with the New Zealand National Seismic Hazard Model
Kuo-Fong Ma	9:45-10:00	1A- 3	Historical earthquakes and dynamic modeling to PSHA
Coffee break & Poster session			
Session 2: Current status of Seismic hazard Assessment for each country (2)			
			Chair : Matt Gerstenberger
Ken Xiansheng Hao	10:50-11:00	1A- 4	Toward Improvement of Seismic Hazard Assessment around Taiwan and Ryukyu trench
Tae-Kyung Hong	11:00-11:15	1A- 5	Aftermath of crustal perturbation and regional seismicity change by the 2011 M9.0 Tohoku-Oki megathrust earthquake
Chung-Han Chan	11:15-11:30	1A- 6	A probabilistic Seismic Hazard Assessment for Taiwan: An update of the Taiwan Earthquake Model in 2019
Nobuyuki Morikawa	11:30-11:45	1A- 7	Recent studies on improvements of models in National Seismic Hazard Maps for Japan
Group photo 1			
Lunch & Poster session			

PM

Session 3: 2018 Hokkaido Eastern Iburi earthquake			
			Chair : Asako Iwaki
[Invited] Saeko Kita	13:00-13:30	1B- 1	Spatial distribution of hypocenters of the 2018 M6.7 Hokkaido Eastern Iburi earthquake and its aftershocks with a three-dimensional seismic velocity structure
Asako Iwaki	13:30-13:45	1B- 2	Broadband ground-motion simulation of the 2018 Hokkaido Eastern Iburi earthquake
Coffee break & Poster session			
Session 4: Active faults and Paleoseismology			
			Chair : Nicol Andy
Nicol Andy	14:30-14:45	1B- 3	Sampling and variability of recurrence intervals for New Zealand surface-rupturing paleoearthquakes; implications for seismic hazard models
Takashi Azuma	14:45-15:00	1B- 4	Active fault survey and long-term evaluation of the Shibetsu fault zone, eastern Hokkaido, Japan
Sze-Chieh Liu	15:00-15:15	1B- 5	Paleo-earthquake records of the Hengchun offshore structure, southern Taiwan
Coffee break & Poster session			
			Group Discussion
			G1: PSHA and model validation (Chung-Han Chan and Matt Gerstenberger)
			G2: Ground motion prediction and site amplification (Hongjun Si and Nobuyuki Morikawa)
			G3: Scenarios and subduction zone modeling (Bill Fry and Yin-Tung Yen)
			G4: Hazard and risk products (Toshihiro Yamada and Elizabet Abbot)
			G5: Fault structure and deformation model (Takashi Azuma and Andy Nicol)
	16:00		
	17:00		Reception & Poster session

Program on 5 November 2019 (Tuesday)

Location: Toyako Cultural Center

AM

Session 5: Seismic hazard and risk				Chair : Ruey-Juin Rau
Konstantinos Konstantinou	9:00-9:15	2A- 1	The seismic future of the metropolitan city of Athens (Greece)	
Toshihiro Yamada	9:15-9:30	2A- 2	The Application and the Technical Issue of PSHA	
Yiwun Liao	9:30-9:45	2A- 3	Analysis of aftershocks sequence of $M \geq 6.0$ earthquakes in Taiwan with ETAS model	
Russ Van Disser	9:45-10:00	2A- 4	Millennial-scale slip rate variations on major strike-slip faults in central New Zealand and examples of potential resulting impacts on hazard estimation	
Coffee break & Poster session				
Session 6: Deformation, Fault displacement				Chair : Russ Van Disser
Ruey-Juin Rau	11:00-11:15	2A- 5	Liquefaction-induced ground deformation caused by the shaking of the 2016 Meinong earthquake	
Ian Hamling	11:15-11:30	2A- 6	In search of New Zealand's hidden faults: towards a high resolution velocity field from InSAR and GPS observations	
Jia-Cian Gao	11:30-11:45	2A- 7	Probabilistic Fault Displacement Hazard Analysis : An Example of the Hualien area	
Ray Chuang	11:45-12:00	2A- 8	Working towards integrating geodetic data into PSHA	
Lunch & Poster session				

PM

Session 7: Current status of Seismic hazard Assessment for each country (3)				Chair : Bill Fry
[Invited] Mark Petersen	13:00-13:30	2B- 1	2018 and 2023 U.S. National Seismic Hazard Models	
[Invited] Marco Pagani	13:30-14:00	2B- 2	Exploring the Main Characteristics of GEM's Global Mosaic of Hazard Models	
Coffee break & Poster session				
Session 8: Earthquake, Ground motion				Chair : Marco Pagani
Hung-Yu Wu	14:45-15:00	2B- 3	Rate and State Seismicity Simulations for Seismic Hazard Analysis in Taiwan	
Caroline Holden	15:00-15:15	2B- 4	Towards ground motion predictions for a large Hikurangi subduction earthquake: lessons from the Kaikōura earthquake	
Takahiro Maeda	15:15-15:30	2B- 5	Broadband ground-motion waveform synthesis utilizing AI-based upsampling technique	
Bill Fry	15:30-15:45	2B- 6	Dense array ambient noise correlations and seismic reflectivity of the megathrust	
Coffee break & Poster session				
	16:15-16:45		Group Discussion G1: PSHA and model validation (Chung-Han Chan and Matt Gerstenberger) G2: Ground motion prediction and site amplification (Hongjun Si and Nobuyuki Morikawa) G3: Scenarios and subduction zone modeling (Bill Fry and Yin-Tung Yen) G4: Hazard and risk products (Toshihiro Yamada and Elizabeth Abbot) G5: Fault structure and deformation model (Takashi Azuma and Andy Nicol)	
Dinner (ON YOUR OWN)				

Program Poster Session

4-5 November 2019 (Monday - Tuesday)

Location: Toyako Cultural Center

Name	Title
Shao-Yi Huang	P- 1 A revisit to the surface expression of the Milun Fault, east Taiwan
Jyr-Ching Hu	P- 2 Long-term fault slip rates and distributed deformation rates in Taiwan orogenic belt by finite-element kinematic model
Yin-Tung Yen	P- 3 Re-evaluation of Earthquake Probability Assessment for the Active Faults in Taiwan
Kuan-Yu Chen	P- 4 The Significant Fault Sources in Northern Taiwan
Ying-Ping Kuo	P- 5 Logic Tree of Fault Models: A Case Study of Hengchun Fault System in Southern Taiwan
En-Jui Lee	P- 6 GPU-accelerated Automatic Microseismic Monitoring Algorithm
Yen-Yu Lin	P- 7 Stress drops for microseismicity in asperity-like dynamic fault models: actual values vs. estimates from spectral fitting and second-moment approaches
Miki Aso	P- 8 Focal Mechanisms of LFEs in Parkfield by the amplitude inversion using synthetic waveforms
Kuo-En Ching	P- 9 Fault slip deficit rate derived from geodetic data for seismic hazard assessment
Ping-Chen Chiang	P- 10 Insight of the surface deformation in the southwestern Taiwan by using PSInSAR technique
Li-Chieh Lin	P- 11 Estimation of Coulomb Stress Changes from GPS Surface Displacements in the Taiwan Region
Strong Wen	P- 12 Seismogenic characteristics of the plate collision zone: Application of the 2018 Hualien earthquake
Yu-Chih Huang	P- 13 Seismic disasters and volcanism associate with shallow velocity structures suggested from ambient seismic noise studies in Tatun Volcano Group and Aso caldera
Jyun-Yan Huang	P- 14 Mapping profiled engineering bedrock in Taiwan from low cost dense microtremor survey
Ying-Nien Chen	P- 15 Long-period surface wave tomography of Taiwan and Seismic interferometry
Atsushi Wakai	P- 16 Modeling of Subsurface Velocity Structures in Sedimentary basins for the Tokai region, Japan, for broadband strong ground motion prediction
Chun-Te Chen	P- 17 Surface topography effects on seismic amplification in Jiu-Jiu peaks of Taiwan
Tae-Kyung Hong	P- 18 An updated model of seismic hazard map for the Korean Peninsula
Hongjun Si	P- 19 Attenuation characteristics of Recent earthquakes occurred in Alaska and Southern California, the United States of America
Satoshi Shimizu	P- 20 Spatial Distribution Databases of Ground Motion for the recent earthquakes in Taiwan, New Zealand, Italy and Japan
Ming-Kai Hsu	P- 21 Assessing building amplification factor in Taiwan using dense building array
Shohei Naito	P- 22 Development of the building damage detection model based on the deep-learning utilizing aerial photographs of the plural earthquakes
Caroline Holden	P- 23 It's Our Fault research programme: building earthquake resilience for the Wellington region
Hiromitsu Nakamura	P- 24 Prototype of capital stock model of private enterprises by industry for all of Japan to predict economic damage by earthquakes and tsunamis
Chia-Han Tseng	P- 25 Study of factors in distribution and probability of landslides triggered by earthquakes in Taiwan
Yoshinori Tokizane	P- 26 Example of long-term volcanic risk assessment in Shikotsu caldera, Hokkaido, Japan

Program on 6 November 2019 (Wednesday)

Location: Hokkaido Toyako Summit Memorial

AM

Chair : Ken Xiansheng Hao, Takahiro Maeda

9:00-11:00	Summary and discussion Presentation from each Group G1: PSHA and model validation (Chung-Han Chan and Matt Gerstenberger) G2: Ground motion prediction and site amplification (Hongjun Si and Nobuyuki Morikawa) G3: Scenarios and subduction zone modeling (Bill Fry and Yin-Tung Yen) G4: Hazard and risk products (Toshihiro Yamada and Elizabeth Abbot) G5: Fault structure and deformation model (Takashi Azuma and Andy Nicol)
Group photo 2	
12:00	Field trip

1A-1 National Seismic Hazard Maps for Japan and its application to improve disaster resilience

^aHiroyuki Fujiwara

^a*National Research Institute for Earth Science and Disaster Resilience, Japan, fujiwara@bosai.go.jp*

The national seismic hazard maps for Japan (NSHMJ) are prepared to estimate strong motions caused by earthquakes that could occur in Japan in the future and show the estimated results on the maps. The hazard maps consist of two kinds of maps. One is a probabilistic seismic hazard map (PSHM) that shows the relation between seismic intensity value and its probability of exceedance within a certain time period. The other one is a scenario earthquake-shaking map (SESM). The 2011 Great East Japan Earthquake (Mw 9.0) was the largest event in the history of Japan. The 2016 Kumamoto earthquake sequence occurred on active faults where strong-motion evaluation was executed based on the long-term evaluation and strong-motion prediction method ‘Recipe’ by the Headquarters for Earthquake Research Promotion, Japan. Based on lessons learned from these earthquake disasters, efforts to revise the seismic hazard assessment for Japan are progressing. In order to promote the use of the national seismic hazard maps, we have developed an open web system to provide information interactively, and have named this system the Japan Seismic Hazard Information Station (J-SHIS). This J-SHIS system provides a web mapping system based on open source software that allows public users to easily view various data by Internet browsers. The system manages various data in an integrated manner, including provide detail information on seismic hazard and site amplification models with a 250m mesh resolution, and the deep subsurface velocity structure models. As a consequence of continuous NSHMJ in the 15-years sustainable mission, the national seismic risk assessment (NSRA) on building damage in Japan was conducted based on an accumulated result of NSHMJ. The NSRA results were significantly affected by building structure and building age. We constructed a sets of NSRA database in a mesh-base of 250m, consists of number of building, building structure with attributes, building age, and population accommodation. We then conducted NSRA for the whole of Japan. We also have developed a real-time earthquake damage estimation system for Japan (J-RISQ) on the basis of the J-SHIS data with the aim of helping organizations establish a first response system as quickly as possible in the event of earthquakes.

1A-2 Recent progress and future plans with the New Zealand National Seismic Hazard Model

^a Matt Gerstenberger

^a *GNS Science, New Zealand, m.gerstenberger@gns.cri.nz*

The New Zealand National Seismic Hazard Model (NSHM) has been formally revised twice in the last 20 years. First in 2002 in a revision that is tied to the current building design standard and second in a 2012 revision that is used in engineering design, for insurance purposes and numerous other societal decisions. Importantly the core assumptions and PSHA methods have largely remained unchanged since 1998. During this period, we have learned a significant amount about earthquake hazards in New Zealand and our knowledge of how to model them has vastly improved. Our recent efforts have been around establishing funding for a short-term revision to get the model to current international standards and then a longer-term cycle of revisions that will integrate with revisions to the building design standards and national-scale risk models. We have identified multiple priorities for the revision that include scientific, procedural and results-delivery improvements. Some of the key topics are: 1) the development of a New Zealand Community Fault Model; 2) accounting for epistemic uncertainty in source modelling, including hybrid models and segmentation (e.g., reduction in reliance on strict segmentation); 3) alternative methods for epistemic uncertainty in ground motion models, including Sammon's mapping; 4) validation of ground motion simulation and understanding of their skill in improving ground motion predictions via data assimilation; 5) end-user participation in the development of the model to optimise it for their needs and exploration of, e.g., the trade-off between increased precision and uncertainty for decision making; 6) use of international participatory review panel; 7) rigorous open documentation; 8) open and web-based results delivery.

1A-3 Historical earthquakes and dynamic modeling to PSHA

^{a, b}Kuo-Fong Ma,

^a*Earthquake-Disaster & Risk Evaluation and Management (E-DREaM) Center, National Central University, Taiwan, ROC, fong@ncu.edu.tw*

^b*Institute of Earth Sciences, Academia Sinica, Taiwan, ROC*

Significant crustal damaging earthquakes in Taiwan mostly were from complicated fault system rather than from a single fault segment, which was not incorporated in the probability on seismic hazard analysis (PSHA) of Taiwan Earthquake Model (TEM), TEM PSHA2015. In addition to the 1999 Chi-Chi Taiwan earthquake, we studied the historical damaging earthquakes as the 1906 M7.1 Meishan earthquake, 1916 M6.8 Nantou earthquake sequence, and the 1935 M7.1 Hsinchu-Taichung earthquakes to understand their seismogenic mechanisms, and, thus, hope to incorporate the knowledge from historical earthquakes for next generation of seismic hazard analysis. For the 1906 Meishan earthquake, our study shows that this earthquake had been resolved to be from a fault system of blind NE strike thrust with EW surface breaching fault (one of the identified seismogenic structures). The 1916 M6.8 Nantou earthquake sequence was resulted from a buried conjugate seismogenic structure above and below the Orogenic wedge. And, the 1935 M7.1 was occurred with bilateral rupture from a blind fault to strike-slip mechanism to the south and thrusting mechanism to the north. We employed the rupture kinematic modeling to the historical geodetic data with comparison to the intensity pattern to understand the possible involvement of the fault system. These historical and past events suggest that a single fault segment evaluation for seismic hazard might be inadequate, and more complicated fault system identification is necessary. From the dynamic modeling of the 1999 Chi-Chi earthquake, our studies show the importance of heterogenous distribution of horizontal stress in magnitude, which controls the style of slip distribution, and thus, might lead to the discrepancy in slip rate estimation along a single fault. The energy partition in radiated energy, fracture energy, and thermal energy of an earthquake energy budget from dynamic modeling might suggest that the large slip near the surface might be from a thermal-dynamic process. This large slip when counted to the slip rate resulted from plate motion would lead to large uncertainty in slip rate estimation along the fault, and, also might be the reason of the discrepancy from the values in geodetic and geological estimated slip rate. We hope to decipher the knowledge we learnt through events to bring in the next development in probability seismic hazard assessment with more complete picture from seismo-tectonics to earthquake seismology for seismic hazard assessment and risk management.

1A-4 Toward Improvement of Seismic Hazard Assessment around Taiwan and Ryukyu trench

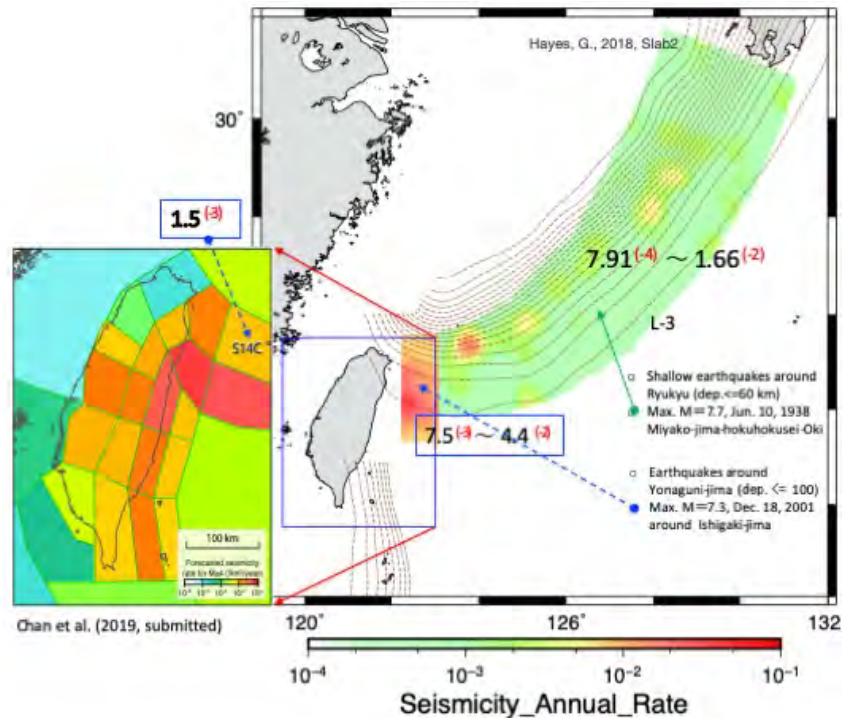
^aKen XianSheng Hao and ^bHiroyuki Fujiwara

^aPrincipal Researcher Fellow, National Institute of Earth Science and Disaster Resilience, Japan, hao@bosai.go.jp

^bDirector, National Institute of Earth Science and Disaster Resilience, Japan, fujiwara@bosai.go.jp

Taiwan located on the south end of Ryukyu trench and on north end of Philippine trench. Larger earthquakes on both of trenches affect the Taiwan. Regional seismic activities almost dominate their result of probabilistic seismic hazard assessment (PSHA). However, beyond Taiwan margin along Ryukyu trench the seismic activity information is limited. A PSHA epistemic uncertainty could be resulted by its short history of literary and instrumental capability on earthquakes. Earthquake catalog used in Taiwan PSHA model is for $M \geq 4.0$ since 1973. On the other hand,

earthquake catalog used in the Ryukyu trench PSHA model is limited only JMA dataset from 1983 for $M \geq 5.0$ that considered instrumental detection capability of observation network. As a consequence, there are differences of the assessment seismicity rates in the two models as shown in the figure. To reduce the PSHA epistemic uncertainty due to the lack of densification seismic data, we propose a Super-Large geotectonic



region to mean the existed annual rate of earthquakes obtained from both of Taiwan and the Ryukyu islands L-3. We are looking forward to work together with Taiwan Earthquake Model to carry on a collaborative research. Thanks Chung-Han Chan's courtesy for the figure.

Keywords: Probabilistic Seismic Hazard Assessment, seismicity, Ryukyu, Taiwan

1A-5 Aftermath of crustal perturbation and regional seismicity change by the 2011 M9.0 Tohoku-Oki megathrust earthquake

^aTae-Kyung Hong, ^bJunhyung Lee, ^cSeongjun Park, ^dIlgoo Kim, and ^eWoohan Kim

^a*Yonsei University, Seoul, South Korea, tkhong@yonsei.ac.kr*

^b*Yonsei University, Seoul, South Korea*

^c*Yonsei University, Seoul, South Korea*

^d*Yonsei University, Seoul, South Korea*

^e*Gyeongsang National University, Jinju, South Korea*

A megathrust earthquake produces large coseismic and postseismic lithospheric displacements. The 2011 M9.0 Tohoku-Oki megathrust earthquakes produced large displacements up to regional distances. The lithospheric displacements directing to the epicenter on the convergent plate boundary developed transient uniaxial tension field over the backarc lithospheres. The V_p/V_s changes display characteristic 2θ azimuthal variations in the upper crust of the Japanese islands, ranging between -0.0458 and 0.0422. Large lateral variations in V_p/V_s changes suggest medium-dependent perturbation. The lower crust of the Korean Peninsula in distances of ~ 1300 km displayed coseismic velocity changes of 3 % after the megathrust earthquake. The V_p/V_s ratios and seismic velocities recovered gradually over time. Peak V_p/V_s and seismic velocity changes were observed along paths subparallel or subperpendicular to the directions toward the megathrust earthquake. The azimuthal seismic anisotropy may have developed from preferential crack orientation and azimuthal lithostatic stress changes. The recovery of the medium properties may take decades. A series of moderate-sized earthquakes occurred as a consequence of medium response to the temporal evolution of stress field in the Korean Peninsula. The distance-dependent coseismic and postseismic displacements caused medium weakening and stress perturbation in the crust, and increased the seismicity with successive M5-level earthquakes in the Korean Peninsula. The average M5-level occurrence rate prior to the megathrust earthquake was $\sim 0.15 \text{ yr}^{-1}$ at a 95 %, and the rate has increased to 0.71 yr^{-1} since the megathrust earthquake. The increased seismic risks may continue until the medium properties and stress field are recovered.

1A-6 A probabilistic Seismic Hazard Assessment for Taiwan: An update of the Taiwan Earthquake Model in 2019

^a Chung-Han Chan, ^{b,c} Kuo-Fong Ma, J. ^d Bruce H. Shyu, ^{e,f} Ya-Ting Lee, ^g Yu-Ju Wang,

^h Yin-Tung Yen, and ⁱ Ruey-Juin Rau

^a *Earth Observatory of Singapore, Nanyang Technological University, Singapore, chchan@ntu.edu.sg*

^b *Earthquake-Disaster & Risk Evaluation and Management (E-DREaM) Center, National Central University, Taiwan, fong@ncu.edu.tw*

^c *Department of Earth Sciences, National Central University, Taiwan*

^d *Department of Geosciences, National Taiwan University, Taiwan, jbhs@ntu.edu.tw*

^e *Earthquake-Disaster & Risk Evaluation and Management (E-DREaM) Center, National Central University, Taiwan*

^f *Department of Earth Sciences, National Central University, Taiwan*

^g *Department of Nuclear Backend Management, Taiwan Power Company, Taiwan*

^h *Sinotech Engineering Consultants, Inc., Taiwan, ytyen@sinotech.org.tw*

ⁱ *Department of Earth Sciences, National Cheng Kung University, Taiwan, raurj@mail.ncku.edu.tw*

The Taiwan Earthquake Model (TEM) has published the first version of Taiwan probabilistic seismic hazard assessment in 2015. That assessment was for the ground motion based on engineering bedrock with regional and subduction inter- and intra-slab seismicity, and individual rupture of the thirty-eight crustal seismogenic structure. This updated assessment considered up to date seismogenic structure database, including six newly identified structures with three-dimensional geometry, an updated earthquake catalogue to 2016, state-of-the-art seismic models, and site amplification factors. Current seismic model includes possibility of earthquake on multiple seismogenic structures with potential for a larger earthquake. To include fault memory on some seismogenic structure sources with earthquake records, we incorporated the Brownian Passage Time model. For the crustal seismicity that cannot be attributed to any specific structure, we modelled their spatial distribution through both area source and smoothing kernel into logic tree.

Our assessments include two versions of hazard maps that based on engineering bedrock and V_s^{30} (shear-wave velocity in the upper most 30 meters) of each calculation site. These two hazard maps would be beneficial to engineering purpose and could be easily accessed by laymen without science and engineering background, respectively. In addition, our database and approach could be further implemented for detailed hazard or risk assessments on infrastructures of interest, such as nuclear power plants.

1A-7 Recent studies on improvements of models in National Seismic Hazard Maps for Japan

^a Nobuyuki Morikawa, ^b Hiroyuki Fujiwara and ^c Jun'ichi Miyakoshi

^a *National Research Institute for Earth Science and Disaster Resilience, Japan, morikawa@bosai.go.jp*

^b *National Research Institute for Earth Science and Disaster Resilience, Japan, fujiwara@bosai.go.jp*

^c *Ohsaki Research Institute, Inc., Japan*

In this paper, we introduce recent studies on improvements of models in National Seismic Hazard Maps for Japan (NSHMJ).

The focal depth (H) of the Hokkaido Iburi Earthquake (M6.7) that occurred in September 2018 was about 40 km, and deeper than the usual crustal earthquakes in Japan. Although it was previously known that some small earthquakes occurred at a depth of about 40 km in that area, central Hokkaido, we did not modeled them in NSHMJ. On the other hand, on the southeast side of that area, apart from the both of shallow crustal and subduction earthquakes based on the 1982 Urakawa-oki earthquake (M7.1, H=40km), we have already modeled background earthquakes with a depth of 25 to 45km. Therefore, we add areas of background earthquakes same as the Urakawa-oki earthquake to the central Hokkaido where seismic activity can be seen up to a depth of about 40km.

A large earthquake (M7.4) that occurred in the Pacific Ocean off Fukushima in November 2016 was a shallow crustal event (H=25km). However, all earthquakes in the Pacific Ocean region have been modeled as subduction earthquakes, plate-boundary and intra-slab earthquakes, in NSHMJ. For this issue, we add new region in the Pacific Ocean region of background shallow crustal earthquakes. And we separate shallow crustal earthquakes from subduction earthquakes.

In order to promote the engineering use of NSHMJ, we estimate the seismic hazard assessment for the response spectrum. In this study, we apply three ground motion prediction equations (GMPEs) individually. There is a large difference in the results depending on the equation. The difference is greatly influenced by the ground motion prediction results with extremely few records such as mega-earthquakes or near-source region. However, one of the most important factors causing such a large difference is that individual databases have been built for each Japanese GMPE, and the definition of ground motion index and processing procedures of waveform records have been not unified.

1B-1[Invited] Spatial distribution of hypocenters of the 2018 M6.7 Hokkaido Eastern Iburi earthquake and its aftershocks with a three-dimensional seismic velocity structure

^a Saeko Kita

^a *Building Research Institute, kita@kenken.go.jp*

Hypocenters of the 2018 M6.7 Hokkaido Eastern Iburi earthquake and its aftershocks were relocated using a three-dimensional seismic structure of Kita et al. [2012] and the JMA earthquake catalog. The relocation results show that the focal depth of the mainshock became 35.4 km and its aftershocks are distributed at depths of approximately 10 to 40 km within the lower crust of the anomalous deep and thickened crust near the uppermost mantle material intrusions in the northwestern edge of the Hidaka collision zone. The anomalous deep and thickened crust is formed due to the collision process of the northeastern Japan and Kuril arcs since Miocene.

Like the two previous large events, the aftershocks of this event incline steeply eastward and appear to be distributed in the deeper extension of the Ishikari-teichi-toen fault zone. The aftershocks at depths of 10 to 20 km are located at the western edge of the high attenuation (low-Qp) zone. These kinds of relationships between hypocenters and materials are the same as the previous M~7 two events (the 1970 and 1982 events in the Hidaka collision zone). The anomalous large focal depths of these large events compared with the average depth limit of inland earthquakes in Japan could be caused by the locally lower temperature in south-central Hokkaido. M7 class inland earthquakes have occurred beneath the Hokkaido collision zone approximately every 40 years, including several 1930s, the 1970 and the 1982 events [Ichikawa, 1971]. This 2018 event is one of the M~7 large inland earthquakes that occurred repeatedly at a recurrence interval of ~40 yrs and is important in the collision process in the Hidaka collision zone.

References

- Ichikawa, M. (1971), Reanalysis of the mechanisms of earthquakes which occurred in and near Japan and statistical studies on the nodal plane solutions obtained, 1926–1968, *Geophys. Mag.*, 35, 207–273.
- Kita, S., A. Hasegawa, J. Nakajima, T. Okada, T. Matsuzawa, and K. Katsumata (2012), High-resolution seismic velocity structure beneath the Hokkaido corner, northern Japan: Arc-arc collision and origins of the 1970 M 6.7 Hidaka and 1982 M 7.1 Urakawa-oki earthquakes, *J. Geophys. Res.*, 117, B12301, doi:10.1029/2012JB009356.

1B-2 Broadband ground-motion simulation of the 2018 Hokkaido Eastern Iburi earthquake

^a Asako Iwaki, ^b Hisahiko Kubo, ^c Nobuyuki Morikawa, ^d Takahiro Maeda,
and ^e Hiroyuki Fujiwara

^a National Research Institute for Earth Science and Disaster Resilience, Japan, iwaki@bosai.go.jp

^b National Research Institute for Earth Science and Disaster Resilience, Japan

^c National Research Institute for Earth Science and Disaster Resilience, Japan, morikawa@bosai.go.jp

^d National Research Institute for Earth Science and Disaster Resilience, Japan, tmaeda@bosai.go.jp

^e National Research Institute for Earth Science and Disaster Resilience, Japan, fujiwara@bosai.go.jp

The 2018 Hokkaido Eastern Iburi earthquake ($M_{JMA}=6.7$) was an inland crustal earthquake at a focal depth of approximately 35 km. This earthquake brought strong ground motion to the southern Hokkaido, causing JMA seismic intensity of 6+ and 7 above the fault and nearby, and 6- in the city of Sapporo.

The seismicity around the source region reaches to deeper region compared to other inland areas in Japan (HERP, 2018). Inland crustal earthquakes at this depth have not been considered by the current ground-motion prediction procedure in Japan. Therefore it is necessary to examine whether the strong ground motion from this earthquake can be modeled by the conventional procedure.

We conducted broadband ground-motion simulation using the characterized source model based on the “recipe” for strong motion prediction (HERP, 2017), aiming to reproduce the observed ground motion. A planner fault is set referring to the fault slip model by Kubo et al. (2019, EPS) in the lower crust, in which the rupture starting point is set to 35 km, and a single asperity is set several km shallower than the rupture starting point on the fault plane. Source parameters are derived by the recipe for inland crustal earthquakes. Broadband ground motion time-series on the engineering bedrock is computed by a hybrid technique of the 3D finite-difference method (Aoi et al. 2004) and the stochastic Green’s function method (Dan and Sato 1998) superposed in time domain at the period of 1 s.

After examining several source and attenuation parameters, it was found that the ground motion computed with higher value of short-period level (A) compared to the empirical relation for the ordinary inland crustal earthquake was more consistent with the observed ground motion. It maybe reflecting the feature of the earthquake source characterized by the depth or the tectonic condition.

Acknowledgments: We used strong motion data provided by JMA, Hokkaido, the city of Sapporo, and NIED.

1B-3 Sampling and variability of recurrence intervals for New Zealand surface-rupturing paleoearthquakes; implications for seismic hazard models

^a Andy Nicol, ^b Russ Van Dissen and ^c Russell Robinson

^a *School of Earth and Environment, University of Canterbury, Christchurch 8020, New Zealand, andy.nicol@canterbury.ac.nz,*

^b *GNS Science, PO Box 30368, Lower Hutt, New Zealand, R.VanDissen@gns.cri.nz*

^c *GNS Science, PO Box 30368, Lower Hutt, New Zealand*

Recurrence intervals (RI) for successive earthquakes on individual faults is a key parameter for seismic hazard analysis. These recurrence intervals are most often recorded by paleoseismic datasets primarily derived from trenching fault scarps and dating displaced stratigraphy. The available data are point samples that record the largest earthquakes on individual faults (in New Zealand $>M_w \sim 6$ to 7.2). They become increasingly incomplete with age and, in some cases, could have been generated by events that ruptured multiple faults. In this talk we will consider how sampling of paleoearthquakes and variations in RI arising from fault interactions impact our understanding of these earthquakes and how they could be better incorporated into seismic hazard models. We will draw upon data and synthetic seismicity models for over 100 New Zealand active faults with average RIs of ~ 130 to 8500 yrs and slip rates of ~ 1 -30 mm/yr. These data and models indicate that RI for individual faults can vary by more than an order of magnitude with coefficient of variations (CoV) of 0.2 to 1 (mean of 0.6 ± 0.2). Elapsed time since the last event is generally less than the average RI on individual faults, suggesting that the faults sampled are in active phases of their earthquake histories and/or that average RI is often overestimated. Such increases in estimated RI would be expected for sample incompleteness which maybe only partly countered by double counting of events due to co-rupture of multiple faults.

Despite these sampling issues RI for the best paleoseismic data and earthquake simulations are described by log-normal or Weibull distributions with long recurrence tails (\sim three times the mean) and provide a basis for quantifying actual RI variability (rather than sampling artefacts). Analysis indicates that CoV of RI is negatively related to fault size (e.g., slip rate). These data are consistent with the notion that fault interaction and associated stress perturbations arising from slip on larger faults are more likely to advance or retard future slip on smaller faults than visa versa. Some of these interactions may occur during earthquakes that rupture many faults.

After sampling artefacts have been accounted for, RI data can be estimated in seismic hazard models using a combination of probability density functions, elapsed times, slip rates and lengths for individual faults.

1B-4 Active fault survey and long-term evaluation of the Shibetsu fault zone, eastern Hokkaido, Japan

^aTakashi Azuma

^a*Geological Survey of Japan/AIST, Japan, t-azuma@aist.go.jp*

We conducted paleoseismological trenching survey on the Shibetsu fault zone in 2018. This fault zone is one of major fault zone in Japan selected by HARP, although no fault parameter, such as slip rate and recurrence intervals, were not recognized. We obtained new data of faulting events in Holocene and the last Pleistocene period of this fault zone by trenching and drilling survey.

Shibetsu fault zone is composed with 4 segment of reverse fault trending NE-SW and is 52 km in length. Topographic analysis based on detailed digital elevation model by LiDAR survey shows a new fault trace on the late Pleistocene fluvial terrace.

We made a paleoseismological trenching on that fault trace with size of 28 m in length, 12 m in width and the maximum depth was 7 m.

We observed black soil, pumice, fine sand and gravels on the trench walls. Black soil has ca. 0.5 m thickness and its upper part was disturbed by cultivation. Two of pumice layers were recognized in the trench. Upper pumice is correlated with Ma-ghi and lower pumice is Ma-l based on mineral composition and refractive index of volcanic glass. Volcanic ash and scoria in fine sand layer were not correlated with recognized tephra in catalog. Lower part of fine sand layer was deformed by freeze-thaw process during the last glacial maximum period.

Amount of displacement of bottom of the lower pumice layer is ca. 15 cm in vertical, whereas height difference of top of gravel layer is 2.6 m in vertical based on drilling data. Samples for ¹⁴C dating were picked up from black soil and fine sand layer. Result of ¹⁴C dating gave the age of the last faulting event as between 13,793 cal BP and 7,939 cal BP.

1B-5 Paleo-earthquake records of the Hengchun offshore structure, southern Taiwan

^a Sze-Chieh Liu, ^b J. Bruce H. Shyu, ^c Yuan-Lu Tsai and ^{de} Chuan-Chou Shen

^a *Department of Geosciences, National Taiwan University, Taiwan, liuszechieh@ntu.edu.tw*

^b *Department of Geosciences, National Taiwan University, Taiwan, jbhs@ntu.edu.tw*

^c *Department of Geosciences, National Taiwan University, Taiwan*

^d *Department of Geosciences, National Taiwan University, Taiwan*

^e *High-precision Mass Spectrometry and Environment Change Laboratory (HISPEC), Department of Geosciences, National Taiwan University, Taiwan*

In the southernmost part of Taiwan, the Western Hengchun Tableland is a prominent topographic feature, with several steps of late Pleistocene marine terraces forming the top of the eastward tilting tableland, and uplifted Holocene coral reefs along the coast. To interpret the formation of this tableland, an inferred Hengchun offshore structure has been proposed as an active structure located offshore to the tableland's west. However, the presence of this structure is still under debate, since no record of paleo-earthquakes related to this structure has been identified. In this study, we utilized fossil coral microatolls as paleo-sea-level indicators to identify possible paleo-earthquake records produced by this structure. The highest level of survival (HLS) of corals is limited by the low tide level. Once living corals grow to this level, the upward growth will stop and they will grow outward instead, forming microatoll morphology with a flat top surface. If microatolls were uplifted and killed by co-seismic uplift, the elevation difference between microatolls and the HLS would represent the amount of uplift, and the age of the coral would constrain the age of the earthquake event. In our field survey, we identified uplifted *Porites* coral colonies at six sites along the coast, and found that they can be separated into several groups. Based on our field survey data and U-Th dating results of uplifted corals, we reconstructed a coastal uplift history of the area, and proposed several paleo-earthquake events in the past 2,500 years. These results enabled us to further understand the seismogenic properties and the possible earthquake recurrence intervals of the Hengchun offshore structure.

2A-1 The seismic future of the metropolitan city of Athens (Greece)

^a K. I. Konstantinou, ^b V. Mouslopoulou, ^c V. Saltogianni

^a*Department of Earth Sciences, National Central University, Jhongli, 320 Taiwan, kkonst@ncu.edu.tw*

^b*Institute of Geodynamics, National Observatory of Athens, POB 20048, 11810 Athens, Greece*

^c*GFZ, Telegrafenberg, 14473 Potsdam, Germany*

The existence of active faults near large cities poses significant risk to the life and property of its inhabitants as well as to its public infrastructure. Here, we investigate the interplay between active faulting, seismicity patterns and interseismic strain accumulation within a radius of 50 km around the metropolitan area of Athens, the capital of Greece. We find that, during the period 2011-2018, a total of 4722 earthquakes occurred, the majority of which had local magnitudes < 3.0 , with only four events being of moderate magnitudes (M_L 4.1-4.3). Precise relative locations, with horizontal and vertical errors of < 1 km and 2 km, respectively, were calculated for 2666 of these events using the double-difference algorithm hypoDD. Earthquake relocation was complemented by geodetic strain-rates that derived from 30 permanent GPS stations and a database of 80 active ($n=26$) or possibly active ($n=54$) faults that derived from analysis of high-resolution (5 m) digital elevation models. Comparison of the above datasets shows that the majority of microseismicity clusters along faults of non-resolvable postglacial activity (~ 16 kyr), while most of the faults which are associated with impressive postglacial scarps and historic seismicity appear to be seismically quiet. Nevertheless, GPS data indicate that both, faults with and without postglacial activity, currently accumulate elastic deformation that ranges, for individual faults, from 0.5 to 1.5 mm/yr. These values are consistent with measurements that derive from the geology and suggest that more than 50% of the mapped faults ($n=52$) are capable of generating earthquakes of magnitudes between 6.0 and 6.5. Thus, in addition to the known active fault sources, the metropolitan area of Athens may accommodate additional seismic sources which, despite the fact that they are mainly characterized by long earthquake-recurrence intervals, are currently associated with intense microseismicity and elastic strain accumulation, signifying the need for future investigations on their seismogenic potential.

2A-2 The Application and the Technical Issue of PSHA

^aToshihiro Yamada

^a *OYORMS Corporation, toshihiro.yamada@oyorms.co.jp*

The result of Probabilistic Seismic Hazard Assessment (PSHA) has been expected to be used more effectively for many purposes, but its application area is still limited as seismic design and seismic risk model for insurance.

In this study, I show the framework of PSHA application (Fig. 1) and explain the usage of the seismic risk analysis result for the risk management in the business area. In addition, I introduce our new challenge with NIED evaluating economic impact by the earthquake using economic model, which is application of the computable general equilibrium (CGE) model and was developed by the Disaster Mitigation Research Center of Nagoya University.

Then, I discuss about the uncertainty of site amplification evaluation methods which are the AVS30 based method, equivalent liner method and nonlinear method, used in PSHA.

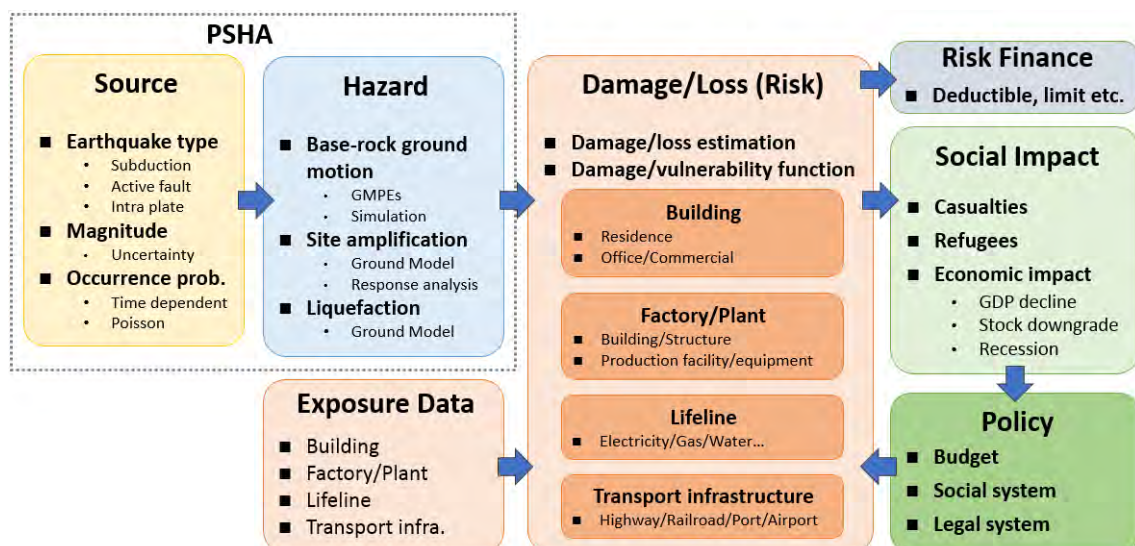


Fig. 1. Framework of PSHA application

2A-3 Analysis of aftershocks sequence of $M \geq 6.0$ earthquakes in Taiwan with ETAS model

^a Yiwun Liao, ^b Jiancang Zhuang, and ^c Kuo-Fong Ma

^a Earthquake-Disaster & Risk Evaluation and Management (E-DREaM) Center of National Central University, Zhongli, Taiwan, yiwun@e-dream.tw

^b The Institute of Statistical Mathematics, Tokyo, Japan

^c Earthquake-Disaster & Risk Evaluation and Management (E-DREaM) Center of National Central University, Zhongli, Taiwan, fong@ncu.edu.tw

It is well known that the earthquake damage is not only from the mainshock, but also from aftershocks, especially for a large significant earthquake. The consequent severe large aftershocks often caused extensive building damages and fatality through the earthquake sequence. To evaluate the hazard and risk from the large aftershocks after a severe earthquake, we analyzed the aftershock sequences of the earthquakes with magnitude larger than 6.0 by using two dimensional point source ETAS (Epidemic-Type Aftershock Sequence) model. To carry out the analysis, we forecasted the spatiotemporal distribution of future aftershocks by considering the aftershock sequence from 1 to 24 hours after the mainshock to investigate the possible lag time for reliable aftershock forecasting (Figure 1 and 2). In our studies, we showed that we can match in general the forecasted spatial distribution of aftershocks with the occurrence pattern of the next-day aftershock sequence by considering the aftershocks in the first few hours after the mainshock through the scoring method. Through these models testing and justification using $M \geq 6.0$ earthquakes in Taiwan, we hope to develop a reliable system for forecasting the spatiotemporal distribution of aftershocks and the time-dependent hazard analysis for future large mainshocks in real-time.

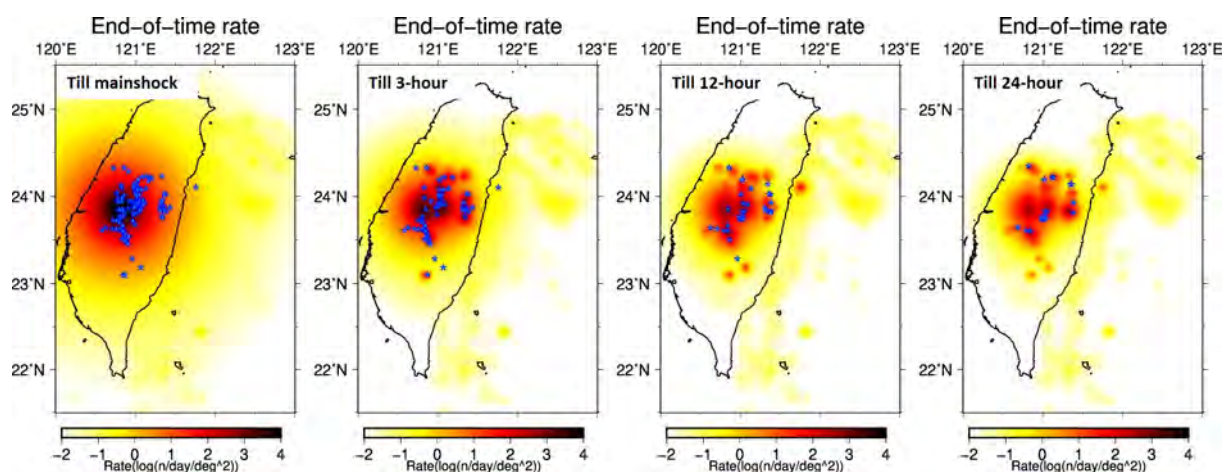


Figure 1. The end-of-time rates of (a) the mainshock, (b) 3-hour, (c) 12-hour, and (d) 24-hour aftershock models.

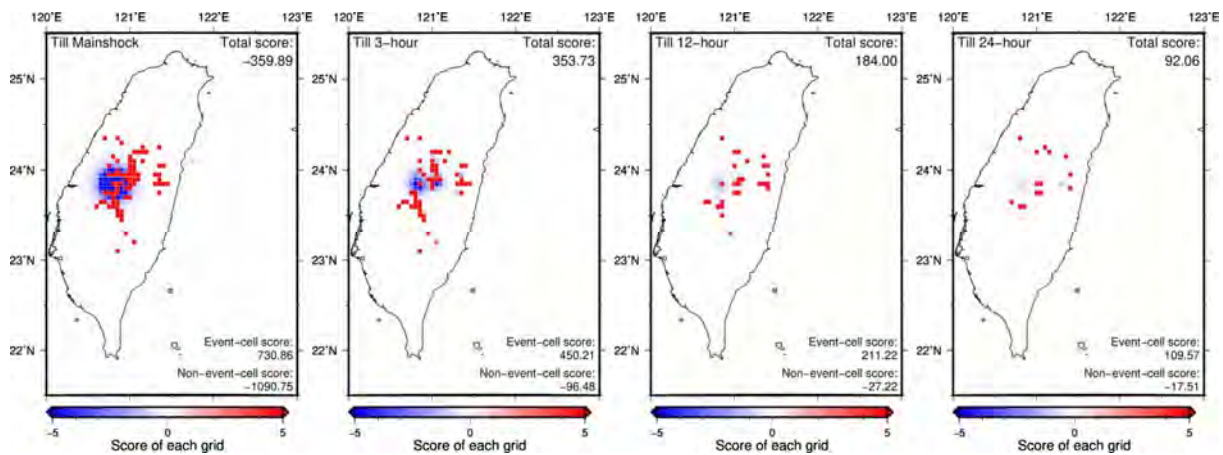


Figure 2. The score distribution of (a) the mainshock, (b) 3-hour, (c) 12-hour, and (d) 24-hour aftershock models.

References

- Ogata, Y., & Zhuang, J. (2006). Space-time ETAS models and an improved extension. *Tectonophysics*, 413(1-2), 13-23.
- Zhuang J. (2006) Second-order residual analysis of spatiotemporal point processes and applications in model evaluation. *Journal of the Royal Statistical Society: Series B (Statistical Methodology)*, 68 (4), 635-653. doi: 10.1111/j.1467-9868.2006.00559.x.
- Zhuang, J. (2011). Next-day earthquake forecasts for the Japan region generated by the ETAS model. *Earth, planets and space*, 63(3), 5.
- Zhuang J., Ogata Y. and Vere-Jones D. (2002). Stochastic declustering of space-time earthquake occurrences. *Journal of the American Statistical Association*, 97: 369-380.
- Zhuang J., Ogata Y. and Vere-Jones D. (2004). Analyzing earthquake clustering features by using stochastic reconstruction. *Journal of Geophysical Research*, 109, No.B5, B05301, doi:10.1029/2003JB002879.

2A-4 Millennial-scale slip rate variations on major strike-slip faults in central New Zealand and examples of potential resulting impacts on hazard estimation

^a Russ Van Dissen, ^b Elizabeth Abbott, ^c Robert Zinke, ^d Dee Ninis, ^e James F. Dolan,

^f Timothy A. Little, ^g Edward J. Rhodes, ^h Nicola J. Litchfield and ⁱ Alexandra E. Hatem

^a GNS Science, New Zealand, r.vandissen@gns.cri.nz

^b GNS Science, New Zealand, e.abbott@gns.cri.nz

^c Jet Propulsion Laboratory, USA

^d Seismological Research Centre, Australia

^e University of Southern California, USA

^f Victoria University of Wellington, New Zealand

^g University of Sheffield, United Kingdom

^h GNS Science, New Zealand

ⁱ United States Geological Survey, USA

Geological investigations over the last decade have demonstrated that major strike-slip faults in central New Zealand (e.g., Awatere, Clarence, Wellington faults) have experienced significant millennial-scale variations in slip rate over the last 10-12 kyr (1 kyr = 1000 years). For example, the central Clarence Fault has had a dextral slip rate of ~2 mm/yr over the last ~8 kyr, whereas, over the preceding ~4 kyr it had a significantly faster rate of ~9 mm/yr. The southern Wellington Fault provides an even more extreme example. Between ~5 kyr and 8 kyr ago, it had a relatively slow slip rate of 1-2 mm/yr, whereas, between ~8 kyr and 10 kyr its slip rate, at nearly 20 mm/yr, was approximately an order of magnitude faster.

In probabilistic seismic hazard assessment, the hazard contribution of an active fault (i.e., an active fault earthquake source) is typically a function of its slip rate, and that slip rate is often assumed to be constant. Here we investigate – in a first-order manner – potential impacts of the above slip rate variations on probabilistic ground shaking hazard estimation. Specifically, we utilise the New Zealand National Seismic Hazard Model and track changes in calculated peak ground acceleration and spectral acceleration that result from slip rate variations on the above faults equivalent in magnitude to those experienced in the past, and plausibly anticipated in the future. We report these changes over a range of annual exceedance probabilities for a representative suite of urban centres in central New Zealand (e.g., Wellington, Blenheim, Kaikoura).

References

- Ninis, D., Little, T.A., Van Dissen, R.J., Litchfield, N.J., Smith, E.G.C., Wang, N., Rieser, U., Henderson, C.M., 2013, Slip rate on the Wellington Fault, New Zealand, during the late Quaternary: Evidence for variable slip during the Holocene. *Bulletin of the Seismological Society of America* 103 (1): 559-579. doi: 10.1785/0120120162.
- Zinke, R., Hollingsworth, J., Dolan, J., Van Dissen, R., 2019, Three-Dimensional surface deformation in the 2016 Mw 7.8 Kaikōura, New Zealand earthquake from optical image correlation: Implications for strain localization and long-term evolution of the Pacific-Australian plate boundary. *Geochemistry, Geophysics, Geosystems* 20 (3): 1609-1628. doi: 10.1029/2018GC007951.

2A-5 Liquefaction-induced ground deformation caused by the shaking of the 2016 Meinong earthquake

^a Ruey-Juin Rau, ^b Choon-Muar Ker, ^c Pei-Ching Tsai, ^d Li-Hsin Ho and ^e Kuo-En Ching

^a *Department of Earth Sciences, National Cheng Kung University, Taiwan, raurj@mail.ncku.edu.tw*

^b *Department of Earth Sciences, National Cheng Kung University, Taiwan*

^c *Department of Earth Sciences, National Cheng Kung University, Taiwan*

^d *Department of Earth Sciences, National Cheng Kung University, Taiwan*

^e *Department of Geomatics, National Cheng Kung University, Taiwan, jingkuen@mail.ncku.edu.tw*

Liquefaction-induced lateral deformations have been commonly observed along the riverbanks and the coastal areas where composed of unconsolidated sediments after nearby moderate or large earthquakes occurred. Liquefaction case history database has been established for liquefaction hazard and potential evaluations, however, there are very few cases in the literatures showing the initiation, evolution and the deformation pattern of liquefaction. The localized Hsinhua, Tainan area in SW Taiwan, had repeatedly experienced liquefaction-induced damages after the nearby moderate (M 6.1-6.6) earthquakes occurred in 1946, 2010 and 2016, respectively. We established 70 campaigned-mode with 400-700 m station-spacing and 9 continuous GPS stations in the Hsinhua area about three months before the 2016 Meinong earthquake, and we made the first campaigned-mode GPS measurements 3-13 days before the event. The campaigned-mode GPS measurements were repeated 2-weeks, six months and one year, respectively after the Meinong earthquake. Each campaign GPS site was occupied 4-8 hours, and the data were calculated by Bernese 5.2 following the standard GPS processing procedures. While the coseismic displacement of the overall Hsinhua area directing mainly northwest-ward, the coseismic displacement within the dense 2x8 km² Hsinhua GPS network shows NW-striking on stations located at two sides of the network and on the contrary, sites intervened in the middle section of the network directing SE. Both the NW- and SE-directing displacements have amplitudes of 20-100 mm. The sites with SE motions form a band with a dimension of 2x5 km² striking NE, normal to the regional coseismic displacement direction. The localized SE-directing area coincides with the InSAR results and roughly consistent with the published liquefaction prone area. In addition to the liquefaction-induced deformation pattern, we will present the initiation and evolution of liquefaction caused by the shaking of the 2016 Meinong earthquake.

2A-6 In search of New Zealand's hidden faults: towards a high resolution velocity field from InSAR and GPS observations

^a I. J. Hamling, ^b T. J. Wright, ^c S. Hreinsdottir, ^{de} L. M. Wallace

^a *GNS Science, New Zealand, i.hamling@gns.cri.nz*

^b *University of Leeds, UK*

^c *GNS Science, New Zealand*

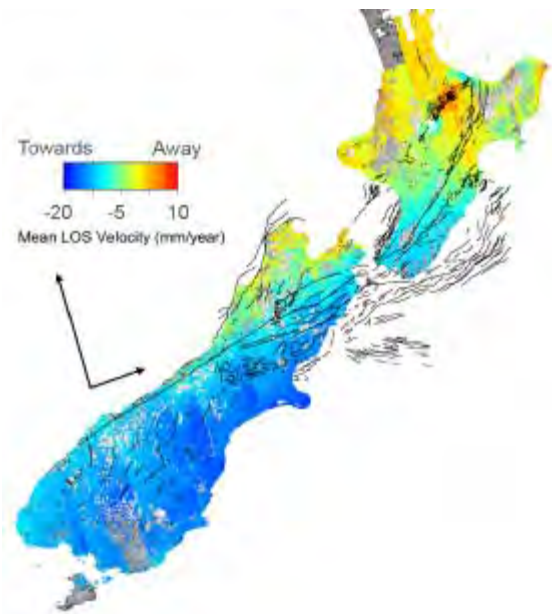
^d *GNS Science, New Zealand*

^e *University of Leeds, UK*

Across New Zealand, the Australian and Pacific plates obliquely converge a rate of 38-49 mm/yr. Variations in the relative plate motions from north to south has led to a transition from the subduction of the Pacific plate beneath the North Island to dextral transpression and strike-slip faulting through the Marlborough Sounds and central South Island. Despite vast improvements in mapping the location of active faults, there have been numerous large damaging earthquakes across New Zealand over the last 10-15 years with many occurring along previously unknown faults. Our current estimates of interseismic strain and long-term fault slip rates have largely been based on modeling of GPS velocities and active fault studies.

The campaign GPS network in New Zealand, which was established in the mid-1990's (with some expansion since then), has benchmarks which are typically located 10-20 km apart (although as dense as 5-10 km in places) and is currently re-measured approximately every eight years. A relatively comprehensive continuous GPS network has operated in much of the North Island (~20-30 km average spacing) for the last 10-15 years, although continuous GPS sites are much sparser in the South Island.

Here, we combine ~10 years of InSAR observations with interseismic campaign and continuous GPS velocities to build a high resolution velocity field of New Zealand. In addition to resolving large scale interseismic deformation, we identify localised deformation associated with small-scale plate locking variations, anthropogenic subsidence, landslides and melting ice.



2A-7 Probabilistic Fault Displacement Hazard Analysis : An Example of the Hualien area

ab Jia-Cian Gao, *cd* Chyi-Tyi Lee, *ef* Kuo-Fong Ma

a Graduate Institute of Applied Geology, National Central University, Taiwan, coolcoke228@gmail.com

b Earthquake-Disaster & Risk Evaluation and Management Center, E-DREaM, Taiwan

c Graduate Institute of Applied Geology, National Central University, Taiwan

d Earthquake-Disaster & Risk Evaluation and Management Center, E-DREaM, Taiwan

e Earthquake-Disaster & Risk Evaluation and Management Center, E-DREaM, Taiwan, fong@ncu.edu.tw

f Department of Earth Sciences, National Central University, Taiwan

Seismic impact to infrastructures may include strong ground-motion impact, fault displacement and ground deformation. Coseismic surface displacements associated with large earthquakes have caused significant damage to structures located on or near a fault and may impact existing structures. A method have been proposed (Youngs et al., 2003) to estimate fault displacement in a similarly probabilistic manner as the probabilistic seismic hazard analysis (PSHA). Probabilistic fault displacement hazard analysis (PFDHA) is one such procedure that provides an estimate of expected levels of slip on a fault due to surface rupture.

An earthquake of Mw 6.4 occurred in the Hualien area of eastern Taiwan on 6 February 2018. It caused surface ruptures in several areas mostly near the Milun Fault in Hualien City. The offset reached its maximum of 30 cm. Thus, we try to select empirical distributions for surface rupture, maximum and average displacement, spatial variability of slip, and other random variables that are the key to implementing PFDHA. We calculated fault displacement hazard and compared the results with the distribution of co-seismic surface ruptures through field surveys.

2A-8 Working towards integrating geodetic data into PSHA

^a Ray Y. Chuang, ^b Kuo-En Ching, ^c Wu-Lung Chang, and ^d Ruey-Juin Rau

^a *Department of Geography, National Taiwan University, Taiwan, raychuang@ntu.edu.tw*

^b *Department of Geomatics, National Cheng Kung University, Taiwan, jingkuen@mail.ncku.edu.tw*

^c *Department of Earth Sciences, National Central University, Taiwan*

^d *Department of Earth Sciences, National Cheng Kung University, Taiwan, raurj@mail.ncku.edu.tw*

Geodetic techniques have shown great ability to monitor surface deformation, providing useful information for estimating fault movement. Geodetic rates, fault-slip rates derived from geodetic data, have been widely used in the geodesy community to characterize seismic potential and strain partitioning. Especially, geodetic data could give us insights into current fault locking and slip deficit at the present earthquake cycle, which should be more sensitive to the next earthquakes. However, current probabilistic seismic hazard assessments (PSHA) do not particularly incorporate either geodetic rates or observations. Therefore, this study aims to discuss how to use geodetic observations for seismic hazard assessments. We first compare geologic and geodetic rates of major active faults in Taiwan. Geodetic rates are derived from three different numerical models. Secondly, we propose a framework to incorporate geodetic data into seismic hazard assessments.

2B-1[Invited] 2018 and 2023 U.S. National Seismic Hazard Models

^a M.D. Petersen and the National Seismic Hazard Model Project

^a *Chief National Seismic Hazard Model Project, U.S. Geological Survey, mpetersen@usgs.gov*

During 2017-2018, the National Seismic Hazard Model (NSHM) was updated by incorporating (1) new median ground motion models, new estimates of their epistemic uncertainties and aleatory variabilities, and new soil amplification factors for the central and eastern U.S., (2) amplification of long-period ground motions in deep sedimentary basins in the Los Angeles, San Francisco, Seattle, and Salt Lake City areas, (3) an updated seismicity catalog, which includes new earthquakes that occurred between 2012 and 2017, and (4) improved computer code and implementation details. Results show significantly increased ground shaking in many (but not all) locations across the central and eastern U.S., including the four urban areas (listed above) that overlie deep sedimentary basins in the western U.S. During 2019-2023 the NSHM will consider additional updates including: 3D simulations in urban areas of Los Angeles and Seattle, additional sedimentary basin amplification models for other urban areas (e.g., coastal plain of eastern and southern U.S., Reno, Las Vegas), non-ergodic ground motion models that reconsider epistemic and aleatory uncertainty, and new geological and geodetic data for faults spread across the U.S. These maps will be considered by the Building Seismic Safety Council, American Society of Civil Engineers, and International Building Code committees for inclusion in upcoming building codes. Due to population growth, more people live and work in areas of high or moderate seismic hazard than ever before, leading to higher risk of undesirable consequences from future ground shaking.

2B-2[Invited] Exploring the Main Characteristics of GEM's Global Mosaic of Hazard Models

^a Marco Pagani, ^b Robin Gee, ^c Kendra Johnson, ^d Julio Garcia-Pelaez, and ^e Richard Styron
^a Seismic Hazard Team, Global Earthquake Model Foundation, Italy, marco.pagani@globalquakemodel.org
^b Seismic Hazard Team, Global Earthquake Model Foundation, Italy
^c Seismic Hazard Team, Global Earthquake Model Foundation, Italy
^d Seismic Hazard Team, Global Earthquake Model Foundation, Italy
^e Seismic Hazard Team, Global Earthquake Model Foundation, Italy

In December 2018, at the end of its second implementation phase, the Global Earthquake Model (GEM) initiative released the first collection of products of the GEM's Global

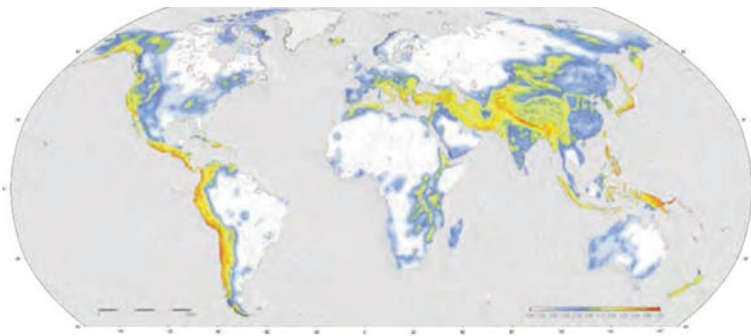


Fig. 1. GEM's Global Hazard Map (Pagani et al, 2019 – v. 2018.1).

earthquake Model suite. These comprise for example a global seismic hazard map (see Figure 1), a global exposure database and a global risk model.

The global hazard map is the combination of 30 hazard maps computed using different regional and national probabilistic seismic hazard models produced by international projects, recognized national agencies and, to a lesser extent, by the GEM Secretariat. Altogether the mosaic provides a good summary of the state-of-practice applied to probabilistic seismic hazard analysis over the last ten years; each model is uniformly described using the OpenQuake Engine input file format (Pagani et al., 2014). Taking advantage of this homogenous representation of the PSHA models, the GEM hazard team is developing a suite of tools to appraise the main characteristics of the Seismic Source and Ground-Motion Characterizations (SSC and GMC, respectively). These tools can appraise the earthquake occurrence characteristics of the different earthquake source typologies used in an SSC or compare the ground motion produced by alternative ground motion models in the SSC for well-specified conditions. In this communication, we provide a summary of the characteristics of the global hazard maps and the mosaic and we illustrate the various comparisons between the hazard models included in the mosaic.

References

- Pagani, M., Monelli, D., Weatherill, G., Danciu, L., Crowley, H., Silva, V., Henshaw, P., Butler, L., Nastasi, M., Panzeri, L., et al. (2014). OpenQuake Engine: An Open Hazard (and Risk) Software for the Global Earthquake Model. *Seismological Research Letters* 85, 692–702.
- Pagani, M., Garcia-Pelaez, J., Gee R., Johnson K., Poggi V., Silva V., Simionato M., Styron R., Vigano' D., Danciu L., Monelli D., and Weatherill G. (2019). The 2018 version of the Global EarthquakeModel: Hazard component. *Earthquake Spectra*, *submitted*.

2B-3 Rate and State Seismicity Simulations for Seismic Hazard Analysis in Taiwan

^a Hung-Yu Wu ^b Kuo-Fong Ma and ^c Bill Fry

^a *Earthquake Disaster & Risk Evaluation and Management Center, National Central University, Taiwan, sonata@eqkc.earth.ncu.edu.tw*

^b *Earthquake Disaster & Risk Evaluation and Management Center, National Central University, Taiwan, fong@ncu.edu.tw*

^c *GNS Science, New Zealand, b.fry@gns.cri.nz*

The seismic hazard analyzes and simulations of in-land large earthquakes are important to evaluate the liability from the study of probabilistic seismic hazard assessment. To understand the occurrence, the probabilities and the dynamic processing of large earthquake, we employed the multi-cycle earthquake simulator RSQSim to exam the fundamental aspects of seismicity distribution in spatial and time. This 3D, boundary element software assembles the friction law and initial stress state to simulate the earthquakes in completely, complex seismogenic system. In this research, we use the CWB earthquake catalog and Taiwan Earthquake Model (TEM) for the RSQSim simulations. The heterogeneous initial stresses and recurrence seismic events would be estimated in ten thousand years. Additionally, these information provide the near optimal nucleation locations and seismic events propagation at the stress evolution in Taiwan faulting systems. Through this process, we would like to examine the model parameters from TEM, and understand the key discrepancy between models and simulators, which will bring the mutual input to TEM for update discussion on slip rate and fault system; and the modification to the model for earthquakes simulator.

2B-4 TOWARDS GROUND MOTION PREDICTIONS FOR A LARGE HIKURANGI SUBDUCTION EARTHQUAKE: LESSONS FROM THE KAIKŌURA EARTHQUAKE

^a Caroline Holden, ^b Yoshi Kaneko and ^c Anna Kaiser

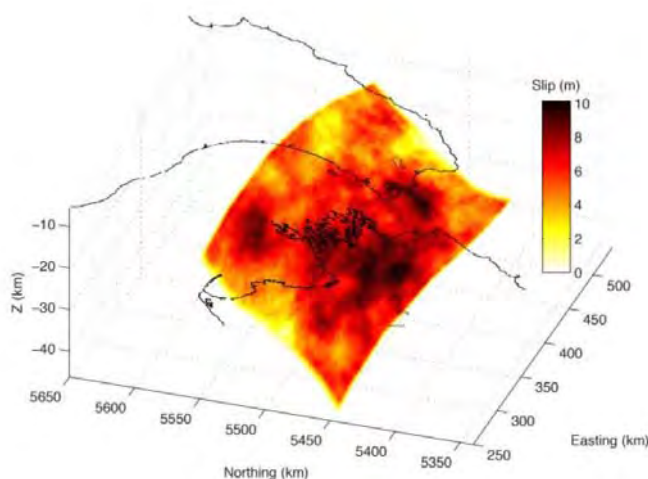
^a GNS SCIENCE, New Zealand, c.holden@gns.cri.nz

^b GNS SCIENCE, New Zealand

^c GNS SCIENCE, New Zealand

The 2016 M7.8 Kaikōura, New Zealand, earthquake struck the East coast of the northern South Island on November 13th 11:02 (UTM). The damaging earthquake generated extreme surface displacements, land deformations and ground motions, a regional tsunami and triggered significant slow slip events on the Hikurangi interface (Kaneko et al., 2017). Sadly, it also caused 2 fatalities and many New Zealanders were affected by this earthquake.

The overall earthquake rupture process as suggested by advanced source models (Hamling et al., 2017; Holden et al., 2017; Kaiser et al., 2017) is complex and unexpected. The earthquake bypassed the Hope fault, largest source of regional seismic hazard, as it ruptured exclusively to the North (despite most of the stress accumulated from the 2010-2016 Canterbury earthquake sequence was to the South). Source models based on teleseismic and/or regional data suggest that the interface did contribute to the overall rupture (Bai et al., 2017; Duputel & Rivera, 2017; Kaiser et al., 2017). However, many observations strongly support evidence of minor (if any) contribution of the interface in the overall rupture (Holden et al., 2017; Clark et al., 2017; Cesca et al., 2017).



These unexpected source characteristics are not considered into best practice (ie seismic hazard models) but significantly impact ground motion results. We entertain a range of realistic source characteristics (Kaneko et al., 2018) of a future Hikurangi earthquake to explore ground motion variability.

Heterogeneous slip on a potential M8.4 Hikurangi subduction earthquake.

Our findings show that strong ground motion is mostly controlled by rupture directivity, stress drop, asperity size, and the presence of sediments and exhibits a large variability despite the tight range of “realistic” parameters employed in our simulations (Holden et al., 2018).

2B-5 Broadband ground-motion waveform synthesis utilizing AI-based upsampling technique

^a Takahiro Maeda, ^b Asako Iwaki, and ^c Hiroyuki Fujiwara

^a *National Research Institute for Earth Science and Disaster Resilience, Japan, tmaeda@bosai.go.jp*

^b *National Research Institute for Earth Science and Disaster Resilience, Japan, iwaki@bosai.go.jp*

^c *National Research Institute for Earth Science and Disaster Resilience, Japan, fujiwara@bosai.go.jp*

For predicting broadband ground motion, a hybrid method is often used. The hybrid method synthesizes broadband ground motion by summing up long-period and short-period ground motion calculated separately. However, the long-period and short-period ground motions are calculated using different velocity structure models, it is known that problems such as the shift of travel time, discontinuity of spectral amplitude between the period range.

For this problem, Iwaki and Fujiwara (2013) proposed a method of synthesizing broadband ground-motion waveform based on the relationship of ground-motion waveform between long-period and short-period extracted from observation data. We considered this problem of extracting the relationship between long-period and short-period ground motions as a problem of upsampling in artificial intelligence (AI) and have studied this problem using the coupling learning method (Nagata et al., 2016) which is one of machine learning methods (Maeda et al., 2018, 2019). To construct a prediction model of a short-period ground-motion waveform from a long-period ground-motion waveform based on AI, we can utilize a vast amount of strong ground motion data recorded by K-NET and KiK-net.

We used an envelope shape of waveforms for narrowband of 0.5-1.0 Hz, 1-2 Hz, 2-4 Hz, 4-8 Hz, 8-16 Hz, and a Fourier amplitude spectrum for evaluating the similarity of observed and predicted broadband ground motion. The data sets used for learning and testing of AI sites with similar ground conditions, (3) records of multiple observation sites due to earthquakes of the similar magnitude, (4) records of multiple observation sites due to earthquake occurring in the same region, and (5) a whole records from (1) to (4). The prediction performance is slightly higher in the case (1). Qualitatively, it is expected that the prediction performance in the case (1) that can take into consideration the site-specific characteristic of ground motion will be significantly higher and the result of this study suggests that there is room for improvement in the similarity evaluation.

Acknowledgments: This work was partially supported by the Council for Science, Technology and Innovation (CSTI) through the Cross-ministerial Strategic Innovation Promotion Program (SIP), titled “Enhancement of societal resiliency against natural disasters” (Funding agency: JST).

2B-6 Dense array ambient noise correlations and seismic reflectivity of the megathrust

^a Bill Fry

^a *GNS SCIENCE, New Zealand, B.Fry@gns.cri.nz*

We stack dense-array ambient noise autocorrelations to probe the Hikurangi Subduction Zone megathrust in central New Zealand. Autocorrelations have been shown to provide depth estimates of strong impedance contrasts in layered media. We compute sub-array autocorrelation functions from 10-station seismometer deployments over the subduction zone. Using dense array techniques greatly enhances the signal-to-noise ratio of the autocorrelations, allowing possible observations of the subduction interface reflector. Sub-arrays were installed one each side of a transition from a region of geodetic coupling to the south and a geodetically defined “unlocked” region to the north. Our experiment is designed to test the hypothesis that persistent strong interface coupling occurs in dry regions of the megathrust whereas weak coupling exists in regions with elevated pore fluids or pore fluid pressures. We would expect high pore fluid pressures at the plate interface to produce larger amplitude reflections of vertically propagating seismic waves, resulting in larger autocorrelation peaks. We observe relatively higher amplitude autocorrelation spikes over the Porongohau region. In this area, the plate interface is about 15km deep. It is an area that is commonly susceptible to triggering of local earthquakes during dynamic stressing of passing waves from distant or regional earthquakes and also triggering of microseismicity during local slow-slip events, presumably from static stressing mechanisms. Of note, the region experienced particularly high seismicity following the 2016 Mw7.8 Kaikoura earthquake. Our deployment captures the year following this event. Our results provide a baseline from which to search for temporal changes in reflectivity of the interface, allowing an approach to monitoring possible changes in pore-fluids throughout the slow-slip / earthquake cycle.

P-1 A revisit to the surface expression of the Milun Fault, east Taiwan

^a Shao-Yi Huang, ^b Jiun-Yee Yen, ^c I-Chin Yen, and ^d Yu-Ting Kuo

^a *Institute of Earth Sciences, Academia Sinica, Taiwan, shao.syh@gmail.com*

^b *Department of natural resources and environmental studies, National Dong Hwa University, Taiwan*

^c *Graduate Institute of Applied Geology, National Central University, Taiwan, ichin.yen@gmail.com*

^d *Institute of Earth Sciences, Academia Sinica, Taiwan*

On February 6, 2018, a moderate earthquake of M_w 6.4 ignited at a shallow depth (~6.3 km) of east Taiwan, resulting in severe damage to downtown Hualien and more than 200 casualties. The strong ground shaking caused collapse and toppling of four buildings in the center of Hualien City and led to outages of power and water for several days. The Milun Fault has a record of recent activity during the 1951 earthquake series and was hence categorized as an active fault with sinistral and reversal components. The 1951 earthquake reached M_w 7.3 and was reported by many journalists and local geologists; that being said, as a lot of the damage occurred in the form of building toppling or collapse and most of the records were documented with relative geographic positions, the recognition of the fault trace became obscured due to the lack of precise coordinates.

The 20180206 earthquake caught us off guard and offered the opportunity to revisit the surface expression and the underground mechanics of the Milun Fault. The earthquake was moderate yet the loss was devastating because the affected area was densely populated. Field measurements show that the Milun Fault generated larger offsets in the north and declined toward south. Development of step-overs were prominent as the fault crossed downtown area, partly explained why the 1951 records were interpreted as three branches in this transpressional section. The repeated occurrence of offsets at many sites demonstrated the high risk of surface ruptures along the fault line, therefore a high resolution and precise mapping focusing on the fault trace is preferably in this case. We learned our lessons and hope this humbling experience can lend itself to build better disaster risk reduction and management plans in the future.

References

- Shao-Yi Huang, Jiun-Yee Yen, Bo-Lin Wu, I-Chin Yen, and Ray Y. Chuang (2019) Investigating the Milun Fault: The coseismic surface rupture zone of the 2018/02/06 M_L 6.2 Hualien earthquake, Taiwan, *Terr. Atmos. Ocean. Sci.*, 30, 311-335, doi: 10.3319/TAO.2018.12.09.03
- Yu-Ting Kuo, Yu Wang, James Hollingsworth, Shao-Yi Huang, Ray Y., Chuang, Chih-Heng Lu, Yi-Chun Hsu, Hsin Tung, Jiun-Yee Yen, and Chung-Pai Chang (2018) Shallow Fault Rupture of the Milun Fault in the 2018 M_w 6.4 Hualien Earthquake: A High-Resolution Approach from Optical Correlation of Pléiades Satellite Imagery, *Seismological Research Letters*, 90, 1, 97-107, doi: 10.1785/0220180227

P-2 Long-term fault slip rates and distributed deformation rates in Taiwan orogenic belt by finite-element kinematic model

^a Jyr-Ching Hu and ^b Yi-Jui Lee

^a Department of Geosciences, National Taiwan University, Taiwan, jchu@ntu.edu.tw

^b Disaster Prevention Technology Research Center, Sinotech Engineering Consultants, INC, Taiwan

This study used kinematic finite element code to estimate the long-term slip rate of faults and the distributed permanent strain rate to assess the seismic hazard model in Taiwan orogenic belt. The community data sets include thirty-three inland active faults and two subduction

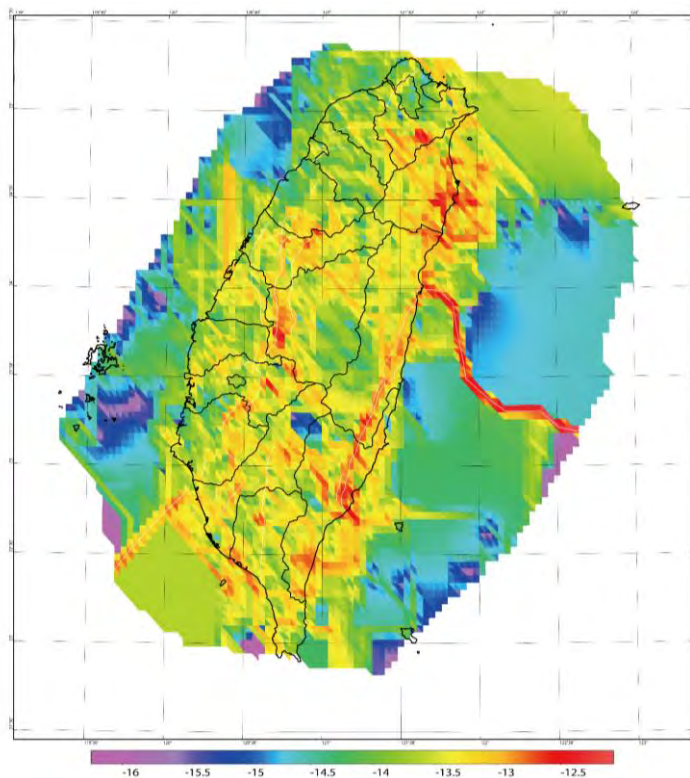


Fig. 1. Distributed permanent strain rates in Taiwan orogenic belt.

plate boundaries. The initial input parameters of each fault include the fault dip, rupture depth and long-term slip rate with consideration of oblique slips on faults. This paper also considered the oblique slips for some active faults. The principal stress direction data obtained from the World Stress Map 2016. We interpolated these stress directions into each finite element. The horizontal GPS velocities which were removed the velocity fields on fault grids and non-tectonic velocities. The plate boundary and Euler pole used the default PB2002 data. The calculation results with compare with the long-term slip rate inferred from two block models in Taiwan and the geological offset rates. The distributed permanent strain rates showed a relatively high strain rate at active faults in southwestern region of Taiwan which the transient deformation contributed by triggering of weak decollement by moderate earthquakes. For instance, the optimized model will be finalized by integrated complete long-term fault slip data and unresolved blind fault systems.

used the default PB2002 data. The calculation results with compare with the long-term slip rate inferred from two block models in Taiwan and the geological offset rates. The distributed permanent strain rates showed a relatively high strain rate at active faults in southwestern region of Taiwan which the transient deformation contributed by triggering of weak decollement by moderate earthquakes. For instance, the optimized model will be finalized by integrated complete long-term fault slip data and unresolved blind fault systems.

P-3 Re-evaluation of Earthquake Probability Assessment for the Active Faults in Taiwan

^a Yin-Tung Yen, ^b Yi-Rui Lee, ^c Yi-Rung Chuang, ^d J. Bruce H. Shyu, ^e Kuo-Shih Shao,
^f Shen-Hsiung Liang, and ^g Chien-Liang Chen

^a *Sinotech Engineering Consultants, Inc., Taiwan, ytyen@sinotech.org.tw*

^b *Sinotech Engineering Consultants, Inc., Taiwan, yirui@sinotech.org.tw*

^c *Sinotech Engineering Consultants, Inc., Taiwan, yrchuang@sinotech.org.tw*

^d *National Taiwan University, Taiwan, jbhs@ntu.edu.tw*

^e *Sinotech Engineering Consultants, Inc., sks@sinotech.org.tw*

^f *Sinotech Engineering Consultants, Inc., shliang@moeacgs.gov.tw*

^g *Sinotech Engineering Consultants, Inc., surveydo@moeacgs.gov.tw*

In the 2013-2016 project “Observation of Fault Activity (III): Integrated Monitoring of Active Faults and Earthquake Probabilities Analysis”, the Central Geological Survey (CGS) has established a procedure for estimating earthquake probabilities for the 33 active faults in Taiwan. The procedure was based on experiences from Japan and the United States to establish a methodology for earthquake probability assessment of existed active faults. Based on the results of this project, the new 2017-2020 project plans to collect the latest parameters and to examine fault geometry model for re-estimating the earthquake probabilities for the active faults in Taiwan. The main tasks of this project are: (1) Re-evaluation of the parameters and earthquake probabilities of the 33 active faults, (2) Collection of the parameters of additional seismogenic structures, (3) Compilation of the parameter explanatory texts, which include fault geometry, activity parameters, and outcrop photos of each active fault, and (4) Analysis of possible issues while publishing the earthquake probability map, and to propose potential coping strategies. The final goal is to provide the potential earthquake probability of each active fault to be appropriately used for calculating earthquake insurance premiums, planning and prioritizing expenditures for seismic upgrades of structures, and the development of building codes.

P-4 The Significant Fault Sources in Northern Taiwan

^aKuan Yu Chen, ^bYi Ping Chen, ^cYing Ping Kuo, ^dAndrew, T. S. Lin, ^eYu Wen Chang, ^fHsun Jen Liu,
^gChih Wei Chang, ^hKevin Clahan, ⁱBor Shouh Huang, ^jChin Tung Cheng and ^kChiun Lin Wu

^a National Applied Research Laboratories-Nation Center for Research on Earthquake Engineering,
 1506020@ncree.narl.org.tw

^b Institute of Oceanography, National Taiwan University, Taiwan

^c National Applied Research Laboratories-Nation Center for Research on Earthquake Engineering,
 ypkuo@ncree.narl.org.tw

^d Department of Earth Sciences, National Central University, Taiwan

^e National Applied Research Laboratories-Nation Center for Research on Earthquake Engineering

^f National Applied Research Laboratories-Nation Center for Research on Earthquake Engineering

^g National Applied Research Laboratories-Nation Center for Research on Earthquake Engineering

^h Lettis consultants international, Inc. Earth science consultants

ⁱ Institute of Earth Sciences of Academia Sinica, Taiwan

^j ThinkTron Ltd., Taiwan

^k National Applied Research Laboratories-Nation Center for Research on Earthquake Engineering

The Seismic Source Characterization (SSC) models are developed by integrating comprehensive data and evaluating various parameters of fault characteristics for probabilistic seismic hazard analysis (PSHA).

The northern Taiwan orogenic belt has collapsed as a result of normal faulting in post-collision stage since late Pliocene-early Pleistocene (Teng, 1996; Hsiao et al, 1998). The submarine reflection seismic data interpretations indicate that the normal faults propagate from offshore area into onshore area (Chen, 2014).

We identified five significant fault sources as primary faults, i.e. Sanchiao fault system, ST-II fault system, Aoti offshore faults, S fault and Northern Ilan fault system. We proposed the logic tree approach to present their geometry (length, dip, and seismogenic depth), kinematics (segmentation and rupture sources), and activity (slip rate, maximum magnitude, magnitude probability distribution function (PDF)) in Northern Taiwan.

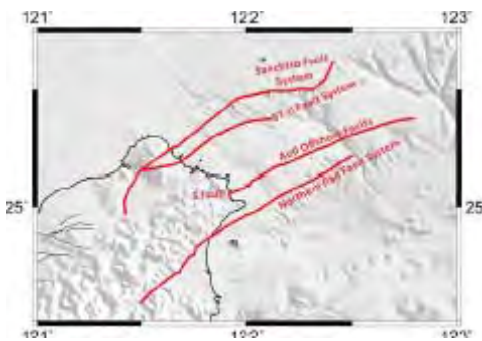


Fig. 1. The significant faults in Northern Taiwan.

References

- Chen, K. Y. (2014) A Study on Structural Development from Orogenic Belt to Extensional Backarc Setting in Northern Taiwan and its Offshore Area. Doctoral Thesis, Department of Earth Sciences, National Central University, Taiwan, pp.199.
- Hsiao, L. Y., Huang, S. T., Teng, L. S. and Lin. K. A. (1998) Structural Characteristics of the Southern Taiwan-Sinzi Folded Zone. *Petroleum Geology of Taiwan*, 32, 133-153.
- Teng, L. S. (1996). Extensional collapse of the northern Taiwan mountain belt. *Geology*, 24(10), 949-952.

P-5 Logic Tree of Fault Models: A Case Study of Hengchun Fault System in Southern Taiwan

^a Ying-Ping Kuo, ^b Kuan-Yu Chen, ^c Yi Ping Chen, ^d Kevin Clahan, ^e Andrew T. S. Lin,
^f Bor Shouh Huang, ^g J. Bruce H. Shyu, and ^h Chiun Lin Wu

^a National Center for Research on Earthquake Engineering, Taiwan, ypkuo@ncree.narl.org.tw

^b National Center for Research on Earthquake Engineering, Taiwan, 1506020@narlabs.org.tw

^c National Taiwan University, Taiwan

^d Lettis consultants international, Inc. Earth science consultants

^e Department of Earth Sciences, National Central University, Taiwan

^f Institute of Earth Sciences of Academia Sinica, Taiwan

^g National Taiwan University, Taiwan, jbhs@ntu.edu.tw

^h National Center for Research on Earthquake Engineering, Taiwan

Taiwan is situated on the boundary between the Philippine Sea Plate and the Eurasian Plate, with a convergence rate of approximately 90 mm/yr. The tectonic of Taiwan orogen is complex and hence is recognized as a high seismicity area. Taiwan SSHAC Level 3 Project is executed by the National Center for Research on Earthquake Engineering (NCREE) to integrate relevant geological/geophysical literature and data, to evaluate the hazard-related parameters, and to establish the logic trees for each seismic source around Taiwan. We evaluated various parameters of fault characteristics by different nodes in logic trees for a site-specific probabilistic seismic hazard analysis (PSHA). One of the four nuclear power plants, NPP3, is located in Hengchun Peninsula, southern Taiwan. The Chaochou fault, the Hengchun fault, the Hengchun offshore fault, and the Southwest Hengchun fault are regarded as Hengchun fault system by the Seismic Source Characteristic Technical Integrator (SSC TI) Team. In this study,

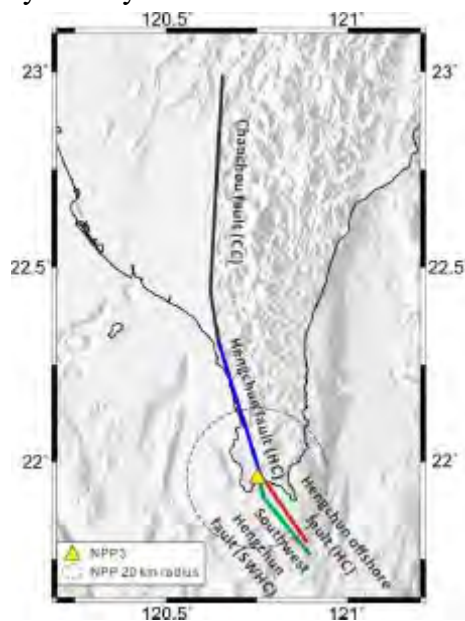


Fig. 1. The map of Hengchun fault system.

Hengchun fault system as being a significant primary fault (located within a 20 km radius of NPP3) would be presented with its final results of the logic tree. The nodes in the logic tree of the Hengchun fault system include geometry [trace, length, depth, dip], kinematics [segmentations, rupture sources], and activity [slip rate, aseismic ratio, maximum magnitude, magnitude PDF].

P-6 GPU-accelerated Automatic Microseismic Monitoring Algorithm

^aEn-Jui Lee, ^bWu-Yu Lioa, ^cDawei Mu, and ^dPo Chen

^a*Department of Earth Sciences, National Cheng Kung University, Taiwan, ROC, rickli92@gmail.com*

^b*Department of Earth Sciences, National Cheng Kung University, Taiwan, ROC*

^c*National Center for Supercomputing Applications, IL, USA*

^d*School of Energy Resources and Department of Geology and Geophysics, University of Wyoming, WY, USA*

We have developed an automatic microseismic monitoring method and have applied to the 2019 Southern California Ridgecrest Earthquake Sequence. The method consists of the following steps: (1) We calculate kurtosis functions of bandpassed continuous seismograms and apply backprojeciton for preliminary earthquake location. (2) We employ a deep learning algorithm to identify P and S arrivals. (3) We then use the preliminary earthquake location and more reliable P and S picks to relocate earthquakes. (4) We adopt the template matching algorithm (TMA) to detect microseismic events in continuous seismic recordings. The algorithm is based on Graphic Processing Units (GPUs) and therefore has been developed for the heavy computational task. The algorithm can provide near real-time microseismic monitoring and therefore able to benefit foreshocks and aftershocks detections of large earthquakes.

P-7 Stress drops for microseismicity in asperity-like dynamic fault models: actual values vs. estimates from spectral fitting and second-moment approaches

^{ab}Yen-Yu Lin and ^{cd}Nadia Lapusta

^a*Department of Earth Sciences, National Central University, Taoyuan, Taiwan, yenyulin@cc.ncu.edu.tw*

^b*Seismological Laboratory, California Institute of Technology, Pasadena, USA*

^c*Seismological Laboratory, California Institute of Technology, Pasadena, USA*

^d*Mechanical and Civil Engineering, California Institute of Technology, Pasadena, USA*

Stress drop, an averaged difference between the shear stress on the fault before and after an earthquake, is an important source parameter. The values estimated by typical seismological methods (e.g., the spectral fitting approaches) suggest that the stress drop is moment-invariant with large scatter and that the on-fault rupture duration t_w obeys the scaling of $t_w \propto M_0^{1/3}$. However, several observations show that microseismic events from the same location can have similar source durations but different seismic moments, violating the commonly assumed scaling. We use numerical simulations of earthquake sequences to demonstrate that strength variations over seismogenic patches provide an explanation of such behavior, with the event duration controlled by the patch size and event magnitude determined by how much of the patch area is ruptured. We find that stress drops estimated by the spectral fitting analyses for the sources simulated in an asperity-like fault model significantly increase with the event magnitude, ranging from 0.006 to 8 MPa. However, the actual stress drops determined from the on-fault stress changes are magnitude-independent at ~ 3 MPa. Our findings suggest that fault heterogeneity results in local deviations in the moment-duration scaling and in earthquake sources with complex shapes of the ruptured area, for some of which stress drops may be significantly (~ 100 - 1000 times) underestimated by the spectral fitting methods. We further apply the stress-drop estimation approach using second moments, which aims to account for rupture directivity and elliptical sources. The second-moment approach indeed works better, providing close estimates of stress drop for sources with rupture areas similar to elliptical ones, but still significantly underestimates, by a factor of up to 30, stress drops for more complex rupture shapes such as ring-like sources. Hence the estimated stress drops still overall increase with the event magnitude, ranging from 0.1 to 2 MPa, but are overall closer to the actual stress drop of ~ 3 MPa.

P-8 Focal Mechanisms of LFEs in Parkfield by the amplitude inversion using synthetic waveforms

^aMiki Aso, ^bNaofumi Aso, ^cSatoshi Ide¹, ^dDavid R. Shelly³

^a *The University of Tokyo*

^b *Tokyo Institute of Technology*

^c *The University of Tokyo*

^d *Geologic Hazards Science Center, U.S. Geological Survey, Golden, CO*

^e *OYO RMS Corporation, miki.aso@oyorms.co.jp*

Various types of earthquakes including ordinary earthquakes and slow earthquakes are observed at the Parkfield section of the San Andreas Fault. Since Shelly et al. (2009) detected low frequency earthquakes (LFEs) at Parkfield, various characteristics have been studied for the 88 LFE families. Thomas et al. (2012) reported the variation in the sensitivities to the tidal stress among LFE families. The stress variation across the San Andreas Fault is also found from the focal mechanisms of ordinary earthquakes; i.e., there are reverse fault earthquakes at several km away from the fault, such as Coalinga earthquake and San Simeon earthquake, while most of the earthquakes are characterized by right-lateral strike slip, which is consistent with plate motion.

In this study, we estimate the focal mechanisms of 88 LFE families in the catalog of Shelly (2017). We first stack seismograms of over one million events in the catalog to improve the signal-to-noise (S/N) ratio. Then, we evaluate the absolute amplitudes of original seismograms using the stacked waveforms. The waveform amplitudes are inverted for the focal mechanisms for each LFE family using synthetic waveforms. Specifically, we first estimate maximum absolute amplitude of three-component waveforms for both stacked and synthetic waveforms, then estimate site effect and focal mechanism by solving an inverse problem. Synthetic waveforms are given by the wavenumber integration method by Zhu and Rivera (2002). As a regional structure, we use 1D structure of velocity and attenuation near Parkfield extracted from Eberhart-Phillips (2016).

As a result, while most of the focal mechanisms are strike-slip consistent with the plate motion at the San Andreas Fault, those for families near central Parkfield and the family off the surface trace contain large dip-slip components. These variations are consistent with the tidal sensitivities of LFEs in Parkfield (Thomas et al., 2012). Our study reveals the regional existence of dip-slip focal mechanisms even along a mature strike-slip fault system.

P-9 Fault slip deficit rate derived from geodetic data for seismic hazard assessment

^a Kuo-En Ching, ^b Wu-Lung Chang, ^c Ray Y. Chuang, ^d Yi-Jui Lee and ^d Yin-Tung Yen

^a *National Cheng Kung University, Taiwan, jingkuen@mail.ncku.edu.tw*

^b *National Central University, Taiwan*

^c *National Taiwan University, Taiwan, raychuang@ntu.edu.tw*

^d *Sinotech Engineering Consultants, Inc., Taiwan*

^c *Sinotech Engineering Consultants, Inc., Taiwan, ytyen@sinotech.org.tw*

How to reasonably estimate fault slip rate using geodetic data is always an important issue for seismic hazard assessment because (1) whether it is reliable to evaluate long-term slip rate based on decadal geodetic observation; (2) the geodetic long-term slip rate is usually one-order higher than geological long-term slip rate especially in Taiwan. In order to solve this issue, a geological rate constraint is usually applied to the block model during the slip rate estimation using geodetic data. In this case, the geodetic long-term slip rate will be highly dependent on the geological slip rate. Therefore, whether geodetic long-term slip rate is really comparable to the geological slip rate? Or could we estimate the reliable geodetic long-term slip rate? If not, which information provided by geodetic data is useful for seismic hazard assessment? Do we need the geological slip rate constraint in a block model? The horizontal and vertical velocity fields in Taiwan were estimated based on the coordinate time series analysis of more than 400 continuous GNSS stations, 700 surveyed-mode GNSS measurements and 29 leveling routes from 2002 to 2018 collected by the Central Geological Survey of Taiwan. These geodetic data were adopted to estimate fault slip rates in western Taiwan. Based on our modeling results in central and northern Taiwan, slip deficit rate is reasonably evaluated in the block model using geodetic data with geological rate constraint instead of the long-term slip rate. In addition, the slip deficit rate is also more comparable with geological slip rate. However, do we really need the geological slip rate constraint to obtain the geodetic slip deficit rate? Based on the further coseismic source models of the 1999 Chi-Chi Taiwan earthquake and the 2015 Gorkha Nepal earthquake, coseismic slip distribution on the decollement is possible. One possible source of the geological and geodetic slip rate difference may hence come from the strain accumulation on decollement. An updating block model is going to be test in western Taiwan to realize the meaning of geological constraint in block model.

P-10 Insight of the surface deformation in the southwestern Taiwan by using PSInSAR technique

^aPing-Chen Chiang, ^bRay Y. Chuang, ^cChih-Heng Lu

^a*Department of Geography, National Taiwan University, Taipei, Taiwan, b04101025@ntu.edu.tw*

^b*Department of Geography, National Taiwan University, Taipei, Taiwan, raychuang@ntu.edu.tw*

^c*Department of Geography, National Taiwan University, Taipei, Taiwan*

The modern geodetic data indicates that the surface deformation of southwestern Taiwan is complicated. Many factors, such as fault movement, tectonic stress, and mud diaper activities, control the horizontal and vertical movement in this area. In addition, after 2016 M_w 6.4 Meinong earthquake shocked the southwestern Taiwan, the spatiotemporal distribution of the aftershocks implies that some blind structures may exist. It is an opportunity to characterize the difference of surface deformation between postseismic and preseismic periods and to understand the time-series surface behaviors. This study processed 105 Sentinel-1 ascending images (27 images are between 2014/10/22 and 2016/02/02 and 78 images are between 2016/02/14 and 2018/12/24) and 76 Sentinel-1 descending images (18 images are between 2014/11/05 and 2016/02/04 and 58 images are between 2016/02/28 and 2018/12/26) with the persistent scatters InSAR (PSI) method to estimate the difference of surface deformation in two periods (Before and after the Meinong earthquake). Furthermore, the PSI results would be verified by GPS data to evaluate the surface deformation of southwestern Taiwan, especially at the Tainan table land and north Kaohsiung.

Keywords: radar, InSAR, surface velocity, crustal deformation

P-11 Estimation of Coulomb Stress Changes from GPS Surface Displacements in the Taiwan Region

^aLi-Chieh Lin, ^bRay Y. Chuang

^a*Department of Geography, National Taiwan University, b05208002@ntu.edu.tw*

^b*Department of Geography, National Taiwan University, raychuang@ntu.edu.tw*

Earthquakes take place when the accumulated stress exceeds the capacity of the surrounding materials can withstand. The failure of the rock materials then releases accumulated energy and cause damage to the vicinity of the epicenter. Therefore, the change of Coulomb Stress can be seen as a possible indicator prior to earthquakes and can well explain the triggering of seismic events. Traditionally, the calculation of Coulomb Stress utilizes a dislocation model assuming a uniform elastic half-space. In this study, we estimate the Coulomb Stress change by using secular GPS surface velocities. With the method used in this study, it provides a more straightforward and easier way to understand the long-term change of Coulomb Stress. By analyzing the change of Coulomb Stress, it may be helpful for earthquake forecasting and minimize the damage which caused by hazardous earthquakes.

Keywords: stress tensor, strain rates, earthquake hazards, seismic potential

P-12 Seismogenic characteristics of the plate collision zone: Application of the 2018 Hualien earthquake

^a Strong Wen, ^bYi-Ying Wen, ^cKuo-En Ching, ^dYu-Lien Yeh, ^eYuan-Hsi Lee

^a *Department of Earth and Environmental Sciences, National Chung Cheng University, Chia-yi County, Taiwan, strong6212@gmail.com*

^b *Department of Earth and Environmental Sciences, National Chung Cheng University, Chia-yi County, Taiwan*

^c *Department of Geomatics, National Cheng Kung University, Tainan, Taiwan, jingkuen@mail.ncku.edu.tw*

^d *Department of Earth and Environmental Sciences, National Chung Cheng University, Chia-yi County, Taiwan*

^e *Department of Earth and Environmental Sciences, National Chung Cheng University, Chia-yi County, Taiwan, leeyuanhsi@gmail.com*

The 2018 Hualien earthquake occurred at the junction of the deformed continental crust of Eurasian plate and the Heping sea basin, where a northeast trending seismic belt exists. In this study, a 3D seismic tomographic inversion is used to investigate the seismogenic structures of the 2018 Hualien earthquake sequence. An earthquake relocation procedure is performed and the focal mechanisms are analyzed to study the faulting behavior. Our results indicate that the source region of the 2018 Hualien earthquake consists of complex high-angle eastward and westward dipping reverse faulting. We also observe that most earthquakes that have occurred in the area exhibit considerable variation in V_p/V_s ratios. Fluid migration may have played an essential role in causing the V_p/V_s ratio variation. Meanwhile, we also analyze the focal mechanisms and conduct stress inversion for these swarms. The results show that these swarms are energetic and short in duration and were dominated by right and left lateral strike-slip events along a prominent lineation in EW and NW directions, respectively. Due to the collision is still active and this compression produces micro-earthquakes likely linked to E-W or NW-SE pre-existing faults which are triggered with oblique-slip faulting. Therefore, the results are not only giving better understanding the seismogenic structure beneath the eastern Taiwan, but also can provide key information to properly assess seismic hazard analysis for the urban area. We suggest that the mainshock of the 2018 Hualien earthquake may be associated with a west-dipping fault, which is a blind fault tending toward the Heping sea basin and possibly belonging to the Central Range fault system.

P-13 Seismic disasters and volcanism associate with shallow velocity structures suggested from ambient seismic noise studies in Tatun Volcano Group and Aso caldera

^a Yu-Chih Huang, ^b Cheng-Horng Lin and ^c Tsuneomi Kagiya

^a National Center for Research on Earthquake Engineering, NARLabs, Taiwan, huangyc@ncree.narl.org.tw

^b Institute of Earth Sciences, Academia Sinica, Taiwan, lin@earth.sinica.edu.tw

^c Aso Volcano Museum, Japan, kagiya.tsuneomi.87w@st.kyoto-u.ac.jp

The magmatic-hydrothermal systems can be investigated through imaging seismic velocity structures, in particular, S-wave velocities (V_s) are generally correlated with hydrothermal fluid or magma distributions. Since the basic theorem of ambient seismic noise has been supported and is routinely used worldwide to investigate subsurface velocity structures. The method uses diffuse wave fields with passive structural signals contained in ambient seismic noise. We try to summarize the obtained shallow velocity structures with the volcanism of Tatun Volcano Group (TVG) in Taiwan and Aso caldera in Japan. We suppose that faults play a significant role with volcanic activity and landslides caused by strong ground shaking during the 2016 Kumamoto and 2018 Hokkaido earthquakes should relate to loose pyroclastic materials at the surface.

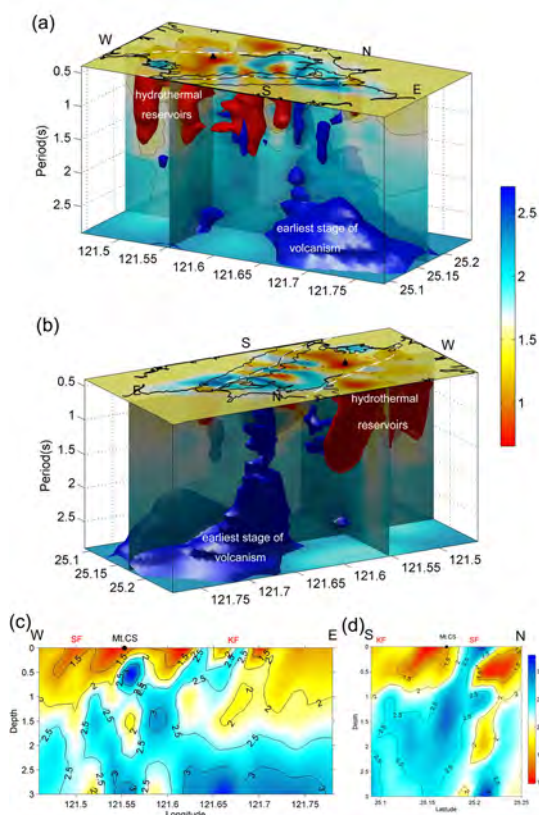


Fig. 1. 3D phase velocity maps and two V_s profiles transect Mt. CS in the shallow 3 km crust. (Huang et al., 2017)

Various recent lines of evidence indicate that TVG is a potentially active volcano, and that the possibility of volcanic eruptions in the future cannot be excluded. Most recent volcanic activities in TVG are concentrated around, and have been observed at Chishingshan (Mt. CS) and Dayoukeng (DYK). Huang et al. (2017) analyzed daily ambient seismic noise of the vertical components from 2014 using a dense seismic network of 40 broadband stations. We investigated shallow crustal phase velocity distributions with a 0.02° grid spacing in the 0.5–3 s period band and two V_s profiles transect Mt. CS to depths of 3 km (Fig. 1). Low velocity zones in the southeast of DYK may be interpreted as hydrothermal reservoirs or water-saturated Tertiary bedrock in the shallow crust. High velocities conspicuously dominate

the east of TVG, where the earliest stages of volcanism in TVG are located, but where surface hydro-geothermal activities were absent in recent times. Between the Shanchiao Fault and Kanchiao Fault high velocities were detected, which converge below Mt. CS. The two faults should play a significant role with the forming and volcanic activity of TVG.

Aso volcano is situated at approximately the center of Kyushu and is one of the most active volcanoes in Japan. Huang et al. (2018) used approximately 4 years of seismic data recorded by a network of 25 seismic stations (i.e., 13 broadband and 12 short-period seismometers) to image Vs structures beneath Aso caldera with seismic noise interferometry. We calculated daily cross-correlation functions (CCFs) of broadband and short-period station pairs separately and then stacked CCFs monthly. Finally, we constructed 1–5-s phase-velocity maps with a 0.05° grid spacing and derived crustal Vs structures at a depth of 6 km (Fig. 2). The post-caldera central cones are characterized by high velocities from the surface to a depth of 1 km. In the center of the post-caldera central cones, low velocities prevail at the surface and extend to major anomalies at depths of 1–2.5 km. These low-velocity anomalies can be assumed to be shallow hydrothermal reservoirs that might be related to surface geothermal activity; it is

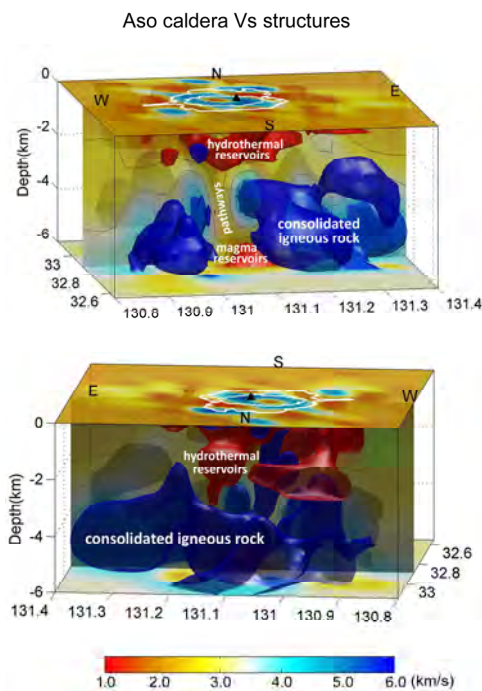


Fig. 2. Two 3-D Vs structures located 6 km beneath Aso caldera. (Huang et al., 2018)

possible that these reservoirs are replenished by precipitation and hydrographic networks within the caldera or through pathways connecting it to deeper earth. The prevalence of high velocities below 3 km can be considered as consolidated igneous rock. Low-velocity anomalies identified at depths of 5–6 km beneath the post-caldera central cones might indicate the tops of magma chambers. The low-velocity belts situated at 2.5–5 km depths are likely pathways for the transfer of hydrothermal fluids, volcanic gases, or melting magma to the surface. The northern part of the caldera exhibits substantial lateral velocity variations, with low velocities and high velocities predominant in the east and west, respectively.

References

- Huang Y. C., C. H. Lin and T. Kagiya (2017), Shallow crustal velocities and volcanism suggested from ambient noise studies using a dense broadband seismic network in the Tatun Volcano Group of Taiwan, *J. Volcanol. Geotherm. Res.*, 341, 6-20.
- Huang Y. C., T. Ohkura, T. Kagiya, S. Yoshikawa and H. Inoue (2018), Shallow volcanic reservoirs and pathways beneath the Aso caldera revealed using ambient seismic noise tomography, *Earth Planets Space*, 70, 169.

P-14 Mapping profiled engineering bedrock in Taiwan from low cost dense microtremor survey

^aJyun-Yan Huang, ^bKuo-Liang Wen, ^cChe-Min Lin and ^dChun-Shiang Kuo

^a*National Center for Research on Earthquake Engineering, Taiwan, jyhuang@narlabs.org.tw*

^b*National Central University, Taiwan, wenkl@ncu.edu.tw*

^c*National Center for Research on Earthquake Engineering, Taiwan, cmlin@narlabs.org.tw*

^d*National Center for Research on Earthquake Engineering, Taiwan, chkuo@ncree.narl.org.tw*

Engineering bedrock was an important issue to consider local site response when studying seismology, the definition was mostly mentioned as the shallower interface of which underlying stratum has from 300 to 700 m/sec of the shear wave velocity. In frequency domain, in contrast, rather than to identify the shear wave velocity 3000- 3500 m/s seismic bedrock, the pre-dominant period of the ground that is close to the proper period of the structures constructed or planned on the mentioned ground is much more important for site response identification. Meanwhile, traditionally shear wave velocity structure inverted from geophysical methods were mostly used to find seismic bedrock and engineering bedrock but basically permanent strong motion stations, lots of earthquake records or proper measurement locations were needed in those methods such as receiver functions, ray tracing, seismic tomography, microtremor array etc. However, single station microtremor measurements were confirmed it could provide dominance frequency map and frequency-dependent site response in map-view for site effect study (Wen and Huang, 2012). It represented the information of deposit thickness and S-wave velocity of the main alluvium layer. Finally, dense microtremor surveys were done in Taiwan after Chi-Chi earthquake, including 3917 measurement sites spreading within sedimentary region such as basin, plain regions. The measurement interval was two to three kilometers in most of the region, and it was five hundred meters to one kilometer in the city. In this study, microtremor measurements were lined up as profiled H/V ratios. The preliminary results indicated high ratio of profiled H/V could link and it was corresponding to main boundary of high velocity contrast layer that was mostly engineering bedrock. Therefore, SungShan formation could be clearly mapping in Taipei basin in this case. The low cost dense microtremor survey could help to identify engineering bedrock for low seismicity country or region to constrain local site effect and might benefit to consider seismic hazard in the near future.

References

Wen K.L. and J.Y. Huang (2012). Dense microtremor survey for site effect study in Taiwan, proceeding of 15 World Conference of Earthquake Engineering (WCEE), Lisboa.

P-15 Long-period surface wave tomography of Taiwan and Seismic interferometry

^aYing-Nien Chen, ^bYuancheng Gung, and ^c Ling-Yun Chiao

^a *Department of Earth and Environmental Sciences, National Chung Cheng University, Taiwan, ynchen@ccu.edu.tw*

^b *Department of Geosciences, National Taiwan University, Taipei, Taiwan.*

^c *Institute of Oceanography, National Taiwan University, Taipei, Taiwan.*

Retrieving empirical Green functions (EGF) between seismic stations by cross-correlating continuous seismic records has quickly become a popular technique in seismology. Based on an implicit high-frequency approximation, the consensus is that the noise cross-correlation function (NCF) of continuous seismic records resembles the Green's Function (GF) of the far-field surface wave between sensors. This perspective leads to the application of the long interstation distance criterion in the dispersion measurements, and, accordingly, much of the low-frequency content in the NCF is rejected. As the spatial extent of Taiwan and the 3-wavelength criterion used in the study of noise are both limiting factors [T.-Y. Huang et al., 2015; Tzu-Ying Huang et al., 2012], the resulting path distribution favors the N-S direction for longer periods. Accordingly, the resolving power for azimuthal anisotropy studies is restricted to shorter periods.

In this study, we show that it is more appropriate to consider the noise cross-correlation function as a product of interference instead of the empirical Green's Function of the far-field surface wave between sensors. We present a new method based on hybrid peak delay time matching to estimate the phase velocities at much lower frequencies of the noise cross-correlation function. Using this method, the dispersion measurement can be extended to much longer periods, allowing the probing of deeper structures with the same noise cross-correlation function dataset. Because there are less limitations on the interstation distance in the approach proposed in this study, the azimuthal coverage of the paths is considerably improved, and the frequency band of the determined dispersion curves is greatly extended to include longer periods.

Reference :

Huang, T.-Y., Y. Gung, W.-T. Liang, L.-Y. Chiao and L. S. Teng (2012). "Broad-band Rayleigh wave tomography of Taiwan and its implications on gravity anomalies." *Geophysical Research Letters* 39(5)

Huang, T.-Y., Y. Gung, B.-Y. Kuo, L.-Y. Chiao and Y.-N. Chen (2015). "Layered deformation in the Taiwan orogen." *Science* **349**(6249): 720-723.

P-16 Modeling of Subsurface Velocity Structures in Sedimentary basins for the Tokai region, Japan, for broadband strong ground motion prediction

^a Atsushi Wakai, ^b Shigeki Senna, ^c Atsushi Yatagai, ^d Haruhiko Suzuki, ^e Yoshiaki Inagaki, ^f Hisanori Matsuyama and ^g Hiroyuki Fujiwara

^a National Research Institute for Earth Science and Disaster Resilience, Japan, wakai@bosai.go.jp

^b National Research Institute for Earth Science and Disaster Resilience, Japan, senna@bosai.go.jp

^c OYO Corporation

^d OYO Corporation

^e OYO Corporation

^f OYO Corporation

^g National Research Institute for Earth Science and Disaster Resilience, Japan, fujiwara@bosai.go.jp

For sophistication of strong ground motion prediction, it is one of the principal issues to model subsurface velocity structures so that earthquake ground motions can be accurately evaluated from 0.1 to 10 s in the broadband period. Therefore, it is indispensable to comprehensively model shallow and deep velocity structures which have ever constructed separately and to constructed subsurface velocity structure models so that earthquake observation records can be reproduced.

In recent years, subsurface velocity structures have been modeled for the Kanto, the Tokai and the Kumamoto region, in a national project.

The modeling procedure [Senna et al., 2019] is as follows. To begin with, initial deep subsurface velocity structures were modeled based on the geological information, the geophysical exploration data and subsurface velocity structure models constructed in the past national investigations. Next, initial shallow velocity structures were modeled based on the existing bore-hole data and surface geological and geomorphologic information which had ever been collected from local governments and so on. Then, through integrating the deep models and the shallow ones in the top surface of engineering basement (the Vs350m/s layer in this study), initial subsurface velocity structures were modeled from the top surface of seismic bedrock to ground surface.

Meanwhile, a lot of ground-motion records were collected through spatially dense and uniform array microtremor measurements and earthquake observations at seismic stations in the target regions. Using ground-motion characteristics such as disperse curves and H/V(R/V) spectral ratios from ground-motion records, each 1-dimensional velocity structure was estimated at each measurement point. With these results, the initial subsurface velocity structure models were improved from the top surface of seismic bedrock to ground surface in the regions.

In this presentation, we will principally report on the modeling process and some features of the improved models for the Tokai region.

References

S. Senna, A. Wakai, A. Yatagai, K. Jin, H. Matsuyama, H. Suzuki and H. Fujiwara (2019), Modeling of the subsurface structure from the seismic bedrock to the ground surface for a broadband strong motion evaluation in Japan, 7th ICEGE Proc. Rome, 17-20 June 2019.

P-17 Surface topography effects on seismic amplification in Jiu-Jiu peaks of Taiwan

^aChun-Te Chen and ^bShiann-Jong Lee

^a*Institute of Earth Sciences, Academia Sinica, Taipei, Taiwan, pokayoke69@gmail.com*

^b*Institute of Earth Sciences, Academia Sinica, Taipei, Taiwan*

A serious large range landslide in Jiu-Jiu peaks area induced by the Chi-Chi earthquake, 1999 in Taiwan. In order to investigate the amplification of seismic response on surface topography. We perform the 3D ground motion simulation in Jiu-Jiu peaks area of Taiwan base on the spectral element method. The 20m resolution Digital Elevation Model (DEM) data was applied to build a mesh model with realistic

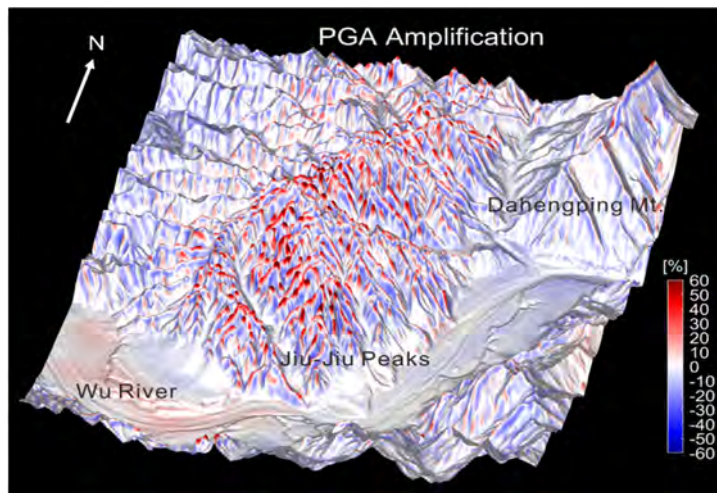


Fig. 1. The PGA amplification of topography effects.

terrain relief. To this end, in a steep topography area like Jiu-Jiu peaks, the designed thin buffer layers are applied to dampen mesh distortion. The three doubling mesh layers near the surface accommodate the finer mesh model. The numerical modeling results show the higher amplification of PGA on the tops and ridges of Jiu-Jiu peaks than surrounding mountains, while the de-amplification most occur near the valley and hillside (Fig 1). In contrast to a flat surface, the relief topography could have a $\pm 50\%$ variation in PGA amplification. The analysis also indicated the topographically amplified seismic response mainly affected the frequency band within 5-10 Hz. However, it worth further investigate the interaction between the realistic topography and the velocity structure on how to impact the seismic response in the different frequency band. The topographically seismic amplification could contribute to a component of innovation in seismic hazard assessment.

terrain relief. To this end, in a steep topography area like Jiu-Jiu peaks, the designed thin buffer layers are applied to dampen mesh distortion. The three doubling mesh layers near the surface accommodate the finer mesh model. The numerical modeling results show the higher amplification of PGA on

P-18 An updated model of seismic hazard map for the Korean Peninsula

^a Seongjun Park, ^b Gyubyeong Rah, and ^c Tae-Kyung Hong

^a *Yonsei University, Seoul, South Korea*

^b *Yonsei University, Seoul, South Korea*

^c *Yonsei University, Seoul, South Korea, tkhong@yonsei.ac.kr*

A probabilistic analysis of seismic hazards is an essential part of natural hazard mitigation for construction of safe society. The Korean Peninsula and its surrounding regions have low seismicity according to the instrumental seismicity since 1978 when the national seismic monitoring began. Historical literatures, however, present many destructive earthquake records, suggesting a potential of large earthquakes. The recent M5-level earthquakes (M5.8, M5.4) raised the public concerns on the potential seismic hazards. A limited number of seismogenic structures were reported. There is difficulty to compile a seismic hazard map with known seismogenic structures. We construct a seismic hazard map of the Korean Peninsula. We collect over 2,000 historical and instrumental events since AD 2. The observed maximum magnitude around the peninsula is M7.0. The background seismicity is assessed using smoothed instrumental seismicity. The Gutenberg-Richter magnitude-frequency relationship is determined to have b value of 0.96. The maximum magnitudes and b values are examined for seismotectonic provinces. We apply various forms of ground motion prediction equations (GMPEs) that were verified through comparison with observed ground motion data. The seismic hazard potentials are high in the southeastern Korean Peninsula and around Pyongyang. The expected peak ground accelerations vary high with input parameters, requesting careful analysis of seismic hazards potentials in the Korean Peninsula.

P-19 Attenuation characteristics of Recent earthquakes occurred in Alaska and Southern California, the United States of America

^a Hongjun Si

^a *Seismological Research Institute Inc., Japan, shj@seismo-r.com*

Recently, three significant earthquakes have occurred in Alaska and Southern California, the USA. Two major earthquakes, the Mw6.5 and the Mw7.0 Ridgecrest earthquakes occurred about 200 km north-northeast of Los Angeles, California, at 10:33:49 on 4 July and 20:19:53 on

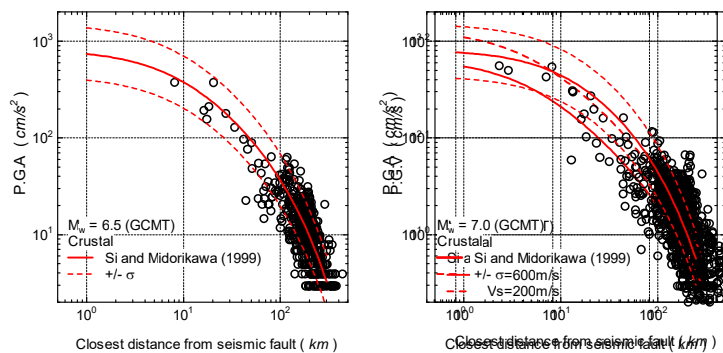


Fig. 1. Comparison of PGAs recorded during the M6.4 and M7.0 2019 Ridgecrest, California earthquakes and the predictions by Si and Midorikawa (1999) based on database in Japan.

the United States. In this study, we compare the attenuation characteristics of the strong ground motions of the two earthquakes with the existing GMPEs developed in Japan and the United States and investigate the spatial distribution of the observed ground motions.

The ground motion data used in this study are those compiled by CESMD. Among these data, the records observed at the stations installed in buildings were excluded. The closest distance from the seismic fault to an observation station is defined as the source distances. PGA and PGV are defined as the larger one among the PGAs and PGVs of the two horizontal components. M_w estimated by GCMT are used in the analysis.

As the preliminary results, we compared the PGAs and PGVs observed during the three earthquakes occurred in the USA and the GMPE by Si and Midorikawa (1999), and found that the observed PGAs for three earthquakes are generally consists with the predictions (Fig. 1).

References

Si, H., Koketsu, K., & Miyake, H. (2019, 08). Preliminary study on the attenuation characteristics of ground motion recorded during the 2019 Ridgecrest earthquakes. Poster Presentation at 2019 SCEC Annual Meeting.

P-20 Spatial Distribution Databases of Ground Motion for the recent earthquakes in Taiwan, New Zealand, Italy and Japan

^a Satoshi Shimizu and ^b Yasushi Komaru

^a *OYO RMS Corporation, Japan, satoshi.shimizu@oyorms.co.jp*

^b *OYO RMS Corporation, Japan, yasushi.komaru@oyorms.co.jp*

The quantitative studies are important to understand and reveal the local risk of earthquake hazard. We estimated the spatial distribution of ground motion for the recent earthquakes in Taiwan, New Zealand, Italy and Japan, including 1999 Chi-Chi earthquake, 2016 Meinong earthquake, 2011 Christchurch earthquake, 2016 Kaikoura earthquake, 2009 L'Aquila earthquake, and 2016 Kumamoto earthquake. The spatial distribution of ground motion at the engineering bedrock was estimated from the observed seismograms by using interpolation after detrending attenuation effect which is called Simple-Kriging method. We use the local seismic network, which is operated by CWB in Taiwan, Geo Net in New Zealand, EMS in Italy, and NIED in Japan. To consider the site amplification, we used the surface velocity V_{s30} published by USGS in Taiwan, New Zealand and Italy, and also using V_{s30} by J-SHIS in Japan. We also used the dense V_{s30} observation by CWB in Taiwan, and combined with USGS data. The fault models were used as a point source or the planer faults published by the previous studies.

We produced the databases of spatial distribution of ground motion as PGA, PGV, JMA Intensity, SI, Sa, and JMA long-period ground motion class. These databases enable to compare the earthquake hazard among countries. They will be released on the website.

P-21 Assessing building amplification factor in Taiwan using dense building array

^a Ming-Kai Hsu, ^bKuo-Fong Ma

^a *Earthquake-Disaster & Risk Evaluation and Management (E-DREaM) Center, National Central University, Taiwan, mingkai@e-dream.tw*

^b *Earthquake-Disaster & Risk Evaluation and Management (E-DREaM) Center, National Central University, Taiwan, fong@ncu.edu.tw*

In this studying we intend to use the densely distributed Palert strong motion stations, which were installed mainly in the first/2nd floor of buildings to evaluate the amplification with dense distribution. We compare the peak ground acceleration (PGA) value between recorded Palert ground-motions and that from ground motion prediction equation (GMPE) to examine the empirical relationship and its possible characteristics from site. Palert network is a high-density low-cost sensor network, which had recording several thousand of records from earthquakes with magnitudes of M_L 2.13 – 6.9 since 2011. Considering the earthquake with different types of focal mechanisms, magnitude and receiving PGA value for each Palert station, we intend to realize the sites effect evaluation in a denser manner to understand the scaling in amplification, which is important for the future evaluation on earthquake scenario modeling from hazard to risk. It is extremely important for the high population metropolitan urbans such as Taipei region in Taipei basin. Through this exercise, we aim to establish the amplification factor map and help the calculation of building damage seismic risk assessment from developed fragility curves, especially with the evaluation on the new definition of intensity scale of 2020.

P-22 Development of the building damage detection model based on the deep-learning utilizing aerial photographs of the plural earthquakes

^a Shohei Naito, ^b Hiromitsu Nakamura and ^c Hiroyuki Fujiwara

^a *National Research Institute for Earth Science and Disaster Resilience, Japan, naito@bosai.go.jp*

^b *National Research Institute for Earth Science and Disaster Resilience, manta@bosai.go.jp*

^c *National Research Institute for Earth Science and Disaster Resilience, fujiwara@bosai.go.jp*

It is important to estimate damage of buildings immediately after the earthquake, for supporting disaster responses performed by the governments and the companies. For this purpose, we developed the immediate damage detection model of buildings based on the deep-learning utilizing the remote sensing images.

We developed the training data by utilizing images of multiple ortho-rectified vertical aerial photos, and each photo was taken soon after the 2016 Kumamoto earthquake, the 1995 southern Hyogo Prefecture earthquake, and the 2011 off the Pacific coast of Tohoku earthquake.

First, we classified damages of all buildings in each photo into four levels by means of the visual judgment; LEVEL1: No damage, LEVEL2: slight damage, LEVEL3: moderate damage, LEVEL4: collapsed. And we organized these damage levels as the GIS data, utilizing the building polygon provided by the Geospatial Information Authority of Japan. Subsequently, we cropped patch images of 80-pixels square which include the main part of a common residence automatically, then extracted approximately 330,000 patches which were labeled by each damage level.

Furthermore, we developed the damage classification model based on the Convolutional Neural Network (CNN) referring the VGG (Simonyan and Zisserman, 2014), and then trained this model with the patches cropped from aerial photos of the plural earthquakes. By utilizing this model, all buildings inside the aerial photograph are automatically classified into four damage levels. Furthermore, as a result of the 10-fold cross validation utilizing the training data generated by Hyogo, Tohoku, and the Kumamoto earthquake, the recalls in each damage level were exceeding 70%. We think such accuracy in four classifications is applicable for the disaster assessments in the context of estimating the prioritization of manpower and resource.

By these methods, the immediate damage detection of the extensive area with an aerial photograph is achieved. Besides, by application of the Bayesian updating method, the estimation result based on the distribution of ground motion can be updated into the higher accuracy.

Additionally, we applied the Bayesian updating method of the J-RISQ (Kusaka et.al, 2017) to the estimation result generated by the CNN-based damage classification model. In the case of the main-shock of the Kumamoto earthquake, the estimation result of J-RISQ was overestimated compared to the governmental field survey result. However, by utilizing the proposed Bayesian updating method with aerial photos, we confirmed the estimation results get closer to the governmental result. For that reason, we think the proposed method is applicable for supporting the disaster responses which is performed by the municipality and the insurance company.

P-23 It's Our Fault research programme: building earthquake resilience for the Wellington region

^a Caroline Holden and ^a Delia Strong

^a *GNS SCIENCE, New Zealand, c.holden@gns.cri.nz*

The It's Our Fault programme started in 2006 to better understand Wellington region's earthquake risk. It is the most comprehensive study of its kind to look at the likelihood and effects of major earthquakes, how these will affect people and infrastructure, and what we can do to prepare and recover. It's Our Fault is jointly funded by EQC (Earthquake Insurance), Wellington City Council and Wellington Region Emergency Management Office.

On behalf of the scientists involved in the project, Caroline will be presenting topics that include hazard studies such as Hikurangi rupture characterization, tsunami and landslide modelling, and planning and policy needs, plus many others supporting evidence-based decision making such as household rainwater tank storage or painting tsunami blue line 'safe zones' on streets in coastal suburbs.



P-24 Prototype of capital stock model of private enterprises by industry for all of Japan to predict economic damage by earthquakes and tsunamis

^a H. Nakamura, ^b H. Fujiwara, ^c I. Takahashi, ^d S. Shimizu, and ^e M. Yamazaki

^a National Research Institute for Earth Science and Disaster Resilience, Japan, manta@bosai.go.jp

^b National Research Institute for Earth Science and Disaster Resilience, Japan, fujiwara@bosai.go.jp

^c National Research Institute for Earth Science and Disaster Resilience, Japan

^d OYO RMS Corporation, Japan, satoshi.shimizu@oyorms.co.jp

^e Nagoya University, Japan

In Cross-ministerial Strategic Innovation Promotion Program (SIP), NIED is developing an economic damage prediction system for the purpose of supporting early economic recovery after the Nankai Trough earthquake.

The system estimates direct and indirect economic damage from earthquakes and tsunamis in all of Japan based on earthquake and tsunami hazard information in real time. It is necessary to calculate the amount of damage to capital stock due to earthquake and tsunami inundation. However, the gross capital stock data of private enterprises by industry is only published at the prefectural level. Therefore, it lacks the spatial resolution necessary for sufficient damage prediction reflecting earthquake and tsunami hazard information.

In this study, we prepared a mesh-level capital stock model of private enterprises by industry of the whole Japan. The capital stock data of private enterprises published by the Cabinet Office was used as the foundation. The spatial resolution was granulized to the city level, district level, and then mesh level. The final capital stock model of private enterprises was obtained for each mesh with 250 m and 50 m sizes for inland and coastal areas, respectively (Fig.1).

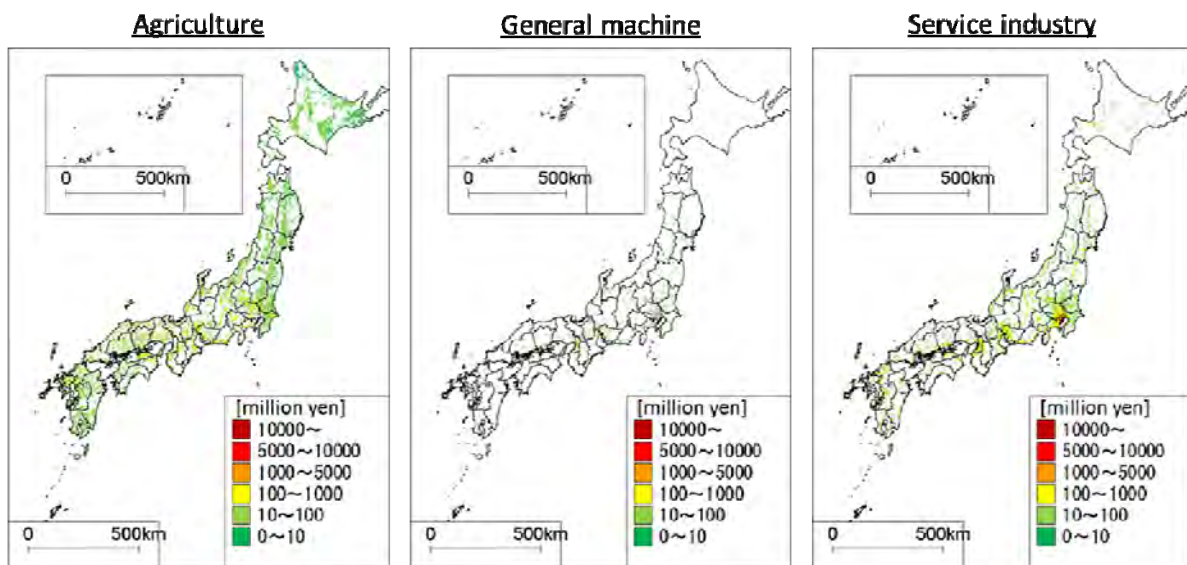


Fig.1 Examples of capital stock model of private enterprises by industry in mesh-level

Acknowledgements

This work was supported by the Council for Science, Technology and Innovation (CSTI) through the Cross-ministerial Strategic Innovation Promotion Program (SIP).

P-25 Study of factors in distribution and probability of landslides triggered by earthquakes in Taiwan

^a Chia-Han Tseng and ^b Ruey-Juin Rau

^a *Graduated Institute of Applied Geology, National Central University, Taiwan, b89204007@gmail.com*

^b *Department of Earth Sciences, National Cheng-Kung University, Taiwan, raurj@mail.ncku.edu.tw*

Taiwan's landscape is characterized by rugged terrains, for exogenic and endogenic processes have both been constantly shaping the terrains since the Taiwan Island was formed. The most destructive exogenic and endogenic processes in Taiwan are torrential rainfalls

brought by either monsoons or typhoons and earthquakes, respectively. They often not only alter the landform in the pattern of mass wasting or landslides, but also consequently make great loss of human lives and property. occurring in 1999.

For the purposes of avoiding and reducing the disaster resulting from landslides, especially triggered by earthquakes, factors which control the distribution and probability of earthquake-triggered landslides are studied. We select the most destructive earthquake event ever recorded in Taiwan, i.e., the Chi-Chi earthquake in 1999 (M_L 7.3), and the landslides triggered by the event (i.e., landslide inventory for the Chi-Chi earthquake (Liao and Lee, 2009)).

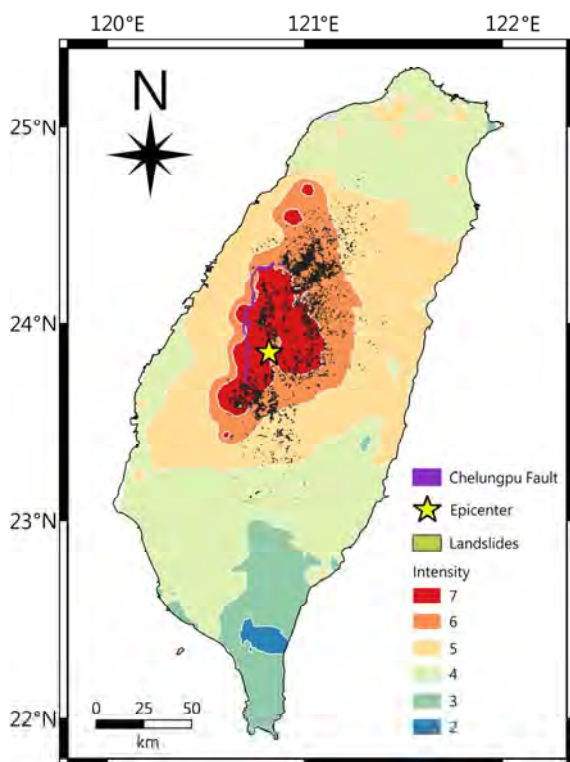


Fig. 1. Distribution of the Chi-Chi Earthquake landslides.

Our preliminary results show that about 90% of the earthquake-triggered landslides are dip slopes (i.e. cataclinal slopes) and occurred within the area where the PGA is larger than 250 gal (i.e. \geq intensity 6; Fig. 1). In addition to the earthquake intensity, other factors which control the distribution and probability of earthquake-triggered landslides, such as distance from the epicenter, distance from the faulting fracture, lithology and slope angle, are also necessary to be discussed for further analyses.

References

Liao H.-W. and C.-T. Lee (2009), Landslides triggered by the Chi-Chi earthquake, <https://www.geospatialworld.net/article/landslides-triggered-by-the-chi-chi-earthquake/>

P-26 Example of long-term volcanic risk assessment in Shikotsu caldera, Hokkaido, Japan

^a Yoshinori Tokizane, ^b Masatsugu Wakaura, ^c Himeka Kikuchi and ^d Toshihiro Yamada

^a OYO RMS Corporation, Japan, yoshinori.tokizane@oyorms.co.jp

^b OYO RMS Corporation, Japan

^c OYO RMS Corporation, Japan, himeka.kikuchi@oyorms.co.jp

^d OYO RMS Corporation, Japan, toshihiro.yamada@oyorms.co.jp

Mt. Tarumae and Eniwa Dake are active volcanoes located in the Shikotsu caldera, Hokkaido (Fig.1). Mt. Tarumae experienced large-scale eruptions in 1667 and 1739. Those eruptions ejected a large amount of pyroclastic fall and pyroclastic flow (Furukawa & Nakagawa, 2010). Shikotsu caldera was formed by the catastrophic eruption in 44ka. The pyroclastic flow deposits at this event widely spread and reached Sapporo city (Yamamoto, 2016), largest city in Hokkaido. In this study, we analyze the risk of ash fall and pyroclastic flow from caused these volcanoes.

We quantify “exposed population” as the risk assessment. We defined that the “exposed population” is the population which is exposed more than 10cm thickness pyroclastic fall deposit or extent of pyroclastic flow. We used logic tree for risk analysis. To evaluate the ash fall hazard, we used the Tephra2 software which is an advection-diffusion simulation. The pyroclastic flow hazard was evaluated using the energy cone model (Fig.2).

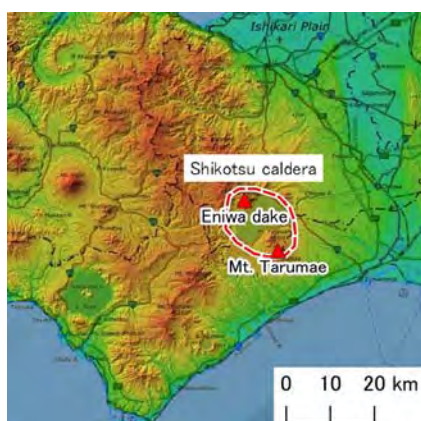


Fig. 1. Location of Shikotsu caldera

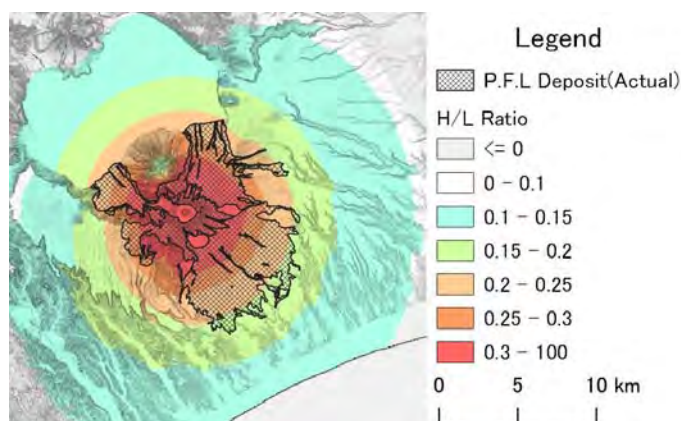


Fig. 2. Result of energy cone model and actual distribution

References

- R. FURUKAWA and M. NAKAGAWA (2010), Geological map of Tarumae volcano, Geological survey of Japan, AIST.
 T. Yamamoto (2016), Volume of erupted magma during the Shikotsu caldera-formation, Hokkaido, Japan. Open-File Report of the Geological Survey of Japan, AIST, No.632, 1-51.